

Frequency combs applications and optical frequency standards^(*)

TH. UDEM⁽¹⁾ and F. RIEHLE⁽²⁾

⁽¹⁾ *Max-Planck Institute für Quantenoptik - Hans-Kopfermann Straße 1, 85748 Garching, Germany*

⁽²⁾ *Physikalisch-Technische-Bundesanstalt - Bundesallee 100, 38116 Braunschweig, Germany*

564	1.	Introduction
565	2.	Frequency combs from mode locked lasers
566	2'1.	Derivation from cavity boundary conditions
568	2'2.	Derivation from the pulse train
571	2'3.	Linewidth of a single mode
573	2'4.	Generating an octave spanning comb
577	3.	Self-referencing
582	4.	Scientific applications
583	4'1.	Hydrogen and drifting constants
586	4'2.	Fine structure constant
587	4'3.	Optical frequencies in astronomy
588	4'4.	Reconstructing pulse transients and generating attosecond pulses
590	4'5.	Frequency comb spectroscopy
593	5.	All optical clocks
595	6.	Optical frequency standards
597	6'1.	Optical frequency standards based on single ions
597	6'1.1.	Clock interrogation by use of quantum jumps
598	6'1.2.	Yb ⁺ and Hg ⁺ single-ion standards
599	6'1.3.	⁸⁸ Sr ⁺ single-ion standard
599	6'2.	Neutral atom optical frequency standards
599	6'2.1.	Atomic beam standards
599	6'2.2.	Neutral atom standards based on ballistic atoms
601	6'2.3.	Optical lattice clocks
602	7.	Conclusions

^(*) Reproduced from Proceedings of the International School of Physics “Enrico Fermi” Course CLXVI “Metrology and Fundamental Constants” edited by T. W. Hänsch, S. Leschiutta, A. J. Wallard and M. L. Rastello (IOS Press, Amsterdam and SIF, Bologna) 2007, pp. 317-365

Summary. — A laser frequency comb allows the conversion of the very rapid oscillations of visible light of some 100's of THz down to frequencies that can be handled with conventional electronics, say below 100 GHz. This capability has enabled the most precise laser spectroscopy experiments yet that allowed to test quantum electrodynamics, to determine fundamental constants and to search for possible slow changes of these constants. Using an optical frequency reference in combination with a laser frequency comb has made it possible to construct all optical atomic clocks, that are about to outperform the current cesium atomic clocks.

1. – Introduction

If one considers the attainable measurement accuracy of different physical quantities it turns out that time intervals and frequencies are to be determined with the utmost precision. Other physical dimensions, such as length mass or charge, can only be determined with orders of magnitude less accuracy. The intrinsic high precision comes about because counting, unlike any other physical measurement, has zero uncertainty connected to it. The only uncertainty in determining a frequency in hertz or oscillations per second, lies in the determination of the second. But this is about as good as it can be, because atomic clocks that are used to determine the second are the most precise instruments. In this sense frequency and time measurements are equivalent.

To exploit this potential it has been a top priority in metrology to convert other physical measurables into a time or frequency equivalent. The simplest example of such a conversion is to assign the speed of light c with a fixed defined value, which was done within the International System of Units (SI) in 1983. Since then the conversion of an optical wavelength λ to an optical frequency $\omega = 2\pi c/\lambda$ can be done without loss of accuracy⁽¹⁾. The method requires a means to count optical frequencies, because only then one can use a precise interferometer to extract the wavelength. Therefore it is no surprise that this redefinition had to wait until it became possible to count the frequency of light. At that time the idea was to calibrate iodine stabilized HeNe lasers with harmonic frequency chains that linked them to a cesium atomic clock. These frequency chains were complex devices that got operational only in few places and worked continuously only for short time intervals [1].

The optical frequency comb vastly simplified these efforts [2-8]. Even commercially available cesium clocks are usually more accurate than an iodine stabilized HeNe laser. Therefore these lasers are no longer required if a more accurate radio frequency (RF) source and a frequency comb is available. On the other hand, another class of optical standards based on trapped ions or atoms have been improving at a faster pace than the cesium clocks so that the frequency comb can be used to calibrate a RF source. As will be discussed in sect. 5 this led to the first all optical atomic clocks [9-11]. After agreeing on a particular ion or atom with a suitable clock transition, it seems likely that

⁽¹⁾ A second example is the utilization of the Josephson effect to convert voltages into frequencies and vice versa.

the definition of the SI second will be adjusted accordingly.

By definition an optical frequency comb consists of many continuous wave laser modes, equidistant in frequency space, that can be used like ruler to determine large frequency differences between lasers. By measuring the frequency separation between a laser at a frequency f and its second harmonic $2f$, the lasers absolute frequency $f = 2f - f$ is determined [12]. A frequency comb used for that purpose must span a complete optical octave. Then, not only f and $2f$ are known relative to the comb mode spacing, but all the modes in between, providing an octave full of calibrated laser lines at once.

Since light from lasers has been used to gather nearly all high-precision data about atoms, the analysis of this light is key to a better understanding of the microscopic world. To test quantum electrodynamics and to determine the Rydberg constant, transition frequencies in atomic hydrogen have been measured [13,14]. In fact the spectroscopy of the narrowest line in hydrogen, the $1S-2S$ transition, was the motivation for setting up the first frequency comb [2-4]. From these measurements the Rydberg constant became the most accurately measured fundamental constant [14]. The frequency comb also helped to determine the fine-structure constant from atomic recoil shifts [15,16] using precise values of the Rydberg constant and was the key for laboratory searches for possible slow variations of these constants [17-19]. Even if there is not yet a physical theory that would predict such a slow change there are some arguments, rather philosophically in nature, that they should be there. The frequency combs are now providing a sharp tool for at least setting up stringent upper limits.

2. – Frequency combs from mode locked lasers

Frequency combs can be produced with fast and efficient electro-optik modulators that impose a large number of side bands on a single-frequency continuous laser [20]. The factor that limited the achievable width of the generated frequency comb was dispersion of the modulator crystal. After dispersion compensation was introduced [21], boosting the intensity with external optical amplifier allowed spectral broadening up to 30 THz bandwidth with the process of self-phase modulation [22].

Even more bandwidth can be generated with a device that already included dispersion compensation, gain and self-phase modulation: the Kerr lens mode-locked laser. Such a laser stabilizes the relative phase of many longitudinal cavity modes such that a solitary short pulse is formed. In the time domain this pulse propagates with its group velocity v_g back and forth between the end mirrors of the resonator. After each round trip a copy of the pulse is obtained at one of these mirrors that is partially transparent like in any other conventional laser. Because of its periodicity, the pulse train generated this way produces a spectrum that consists of discrete modes that can be identified with the longitudinal cavity modes. The process of Kerr lens mode locking (KLM) introduced in the early 90s [23], allows to generate pulses of 10 femtoseconds (fs) duration and below in a rather simple way. For Fourier-limited pulses the bandwidth is given by the inverse of the pulse duration, with a correction factor of order unity that depends on the pulse shape and the way spectral and temporal widths are measured [24]. A 10 fs for example will have a bandwidth of about 100 THz, which is close to the optical carrier frequency, typically at 375 THz (800 nm) for a laser operated near the gain maximum of titanium-sapphire, the most commonly used gain medium in these lasers. By virtue of the repeating pulses, this broad spectrum forms the envelope of a frequency comb. Depending on the length of the laser cavity, that determines the pulse round trip time, the pulse repetition rate ω_r is typically on the order of 100 MHz but 4 MHz through 2 GHz repetition rates have

been used. In any case ω_r is a radio frequency readily measured and stabilized. The usefulness of this comb critically depends on how constant the mode spacing is across the spectrum and to what precision it agrees with the readily measurable repetition rate. These questions will be addressed in the next two sections.

2.1. Derivation from cavity boundary conditions. – As in any laser the modes with wave number $k(\omega_n)$ and frequencies ω_n must obey the following boundary conditions of the resonator of length L :

$$(1) \quad 2Lk(\omega_n) = n2\pi.$$

Here n is a large integer number that measures the number of half wavelengths within the resonator. Besides this propagation phase shift there might be additional phase shifts, caused for example by diffraction (Guoy phase) or by the mirror coatings that are thought of being included in the above dispersion relation. This phase shift may depend on the wavelength of the mode, *i.e.* on the mode number n , and is not simple to determine accurately in practice. So we are seeking a description that lumps all the low-accuracy quantities into readily measurable radio frequencies. For this purpose dispersion is best be included by the following expansion of the wave vector about some mean frequency ω_m , not necessarily a cavity mode according to eq. (1):

$$(2) \quad 2L \left[k(\omega_m) + k'(\omega_m)(\omega_n - \omega_m) + \frac{k''(\omega_m)}{2}(\omega_n - \omega_m)^2 + \dots \right] = 2\pi n.$$

The mode separation $\Delta\omega \equiv \omega_{n+1} - \omega_n$ is obtained by subtracting this formula from itself with n being replaced by $n + 1$:

$$(3) \quad 2L \left[k'(\omega_m)\Delta\omega + \frac{k''(\omega_m)}{2} ((\omega_{n+1} - \omega_m)^2 - (\omega_n - \omega_m)^2) + \dots \right] = 2\pi.$$

To obtain a constant mode spacing, as the most important requirement for optical frequency combs, $\Delta\omega$ must be independent of n . This is the case if and only if all contributions of the expansion of $k(\omega)$ beyond the group velocity term $k'(\omega_m) = 1/\bar{v}_g(\omega_m)$ exactly vanish. The unwanted perturbing terms, or “higher-order dispersion” terms, that contradict a constant mode spacing are those that deform the pulse as it travels inside the laser resonator. Therefore the mere observation of a stable undeformed pulse envelope stored in the laser cavity leads to a frequency comb with constant mode spacing given by

$$(4) \quad \Delta\omega = 2\pi \frac{\bar{v}_g}{2L} \quad \text{with} \quad \bar{v}_g = \frac{1}{k'(\omega_m)}$$

with the round trip averaged group velocity⁽²⁾ given by \bar{v}_g . Having all derivatives beyond $k'(\omega_m)$ vanishing, means that $k'(\omega_m)$ and \bar{v}_g must be independent of frequency. Therefore this derivation is independent of the particular choice of ω_m , provided it resides within

⁽²⁾ The usual textbook approach ignores dispersion either as a whole ($\Delta\omega = 2\pi c/2L$) or just includes a constant refractive index: $\Delta\omega = 2\pi v_{\text{ph}}/2L$ with v_{ph} and c being the phase velocities with and without dispersive material, respectively.

the laser spectrum. The group velocity determines the cavity round trip time T of the pulse and therefore the pulse repetition rate $\omega_r = \Delta\omega$:

$$(5) \quad T^{-1} = \frac{\bar{v}_g}{2L} = \frac{\omega_r}{2\pi}.$$

The frequencies of the modes ω_n of any frequency comb with a constant mode spacing ω_r can be expressed by [3, 8, 25, 26]

$$(6) \quad \boxed{\omega_n = n\omega_r + \omega_{\text{CE}}}$$

with a yet unknown frequency offset ω_{CE} common to all modes. As a convention we will now number the modes such that $0 \leq \omega_{\text{CE}} \leq \omega_r$. This means that ω_{CE} , like ω_r resides in the radio frequency domain. Using (6) to measure the optical frequencies ω_n requires the measurement of ω_r , ω_{CE} and n . The pulse repetition rate can be measured anywhere in the beam of the mode-locked laser. To determine the comb offset requires some more effort as will be detailed in sect. 3. In practice the beam of a continuous wave laser whose frequency is should be determined is superimposed with the beam containing the frequency comb on a photo detector to record a beat note with the nearest comb mode. Knowing ω_r and ω_{CE} the only thing missing is the mode number n . This may be determined by a coarse and simple wavelength measurement or by repeating the same measurement with slightly different repetition rates [27].

Some insight on the nature of the frequency offset ω_{CE} is obtained by resolving (6) for ω_{CE} and using the cavity averaged phase velocity of the n -th mode $\bar{v}_p(\omega_n) = \omega_n/k(\omega_n)$. With the expansion of the wave vector in (2) and the fact that that it ends with the group velocity term, one derives

$$(7) \quad \omega_{\text{CE}} = \omega_n - n\omega_r = \omega_m \left(1 - \frac{\bar{v}_g}{\bar{v}_p(\omega_m)} \right)$$

For this the frequency offset is independent of n , *i.e.* common to all modes, and vanishes if the cavity averaged group and phase velocities are identical. In such a case the pulse train possesses a strictly periodic field that produces a frequency comb containing only integer multiples of ω_r . In general though this condition is not fulfilled and the comb offset frequency is related to the difference of the group and phase round trip time. For an unchirped pulse, that has a well-defined carrier frequency ω_c , it makes sense to expand the wave vector about $\omega_m = \omega_c$ so that eq. (7) becomes

$$(8) \quad \omega_{\text{CE}}T = \Delta\varphi \quad \text{with} \quad \Delta\varphi = \omega_c \left(\frac{2L}{\bar{v}_g} - \frac{2L}{\bar{v}_p} \right).$$

As discussed in more detail in the next section, it follows that the pulse envelope continuously shifts relative to the carrier wave in one direction. The shift per pulse round trip $\Delta\varphi$ is given by the advance of the carrier phase during a phase round trip time $2L/\bar{v}_p$ in a frame that travels with the pulse. The shift $\Delta\varphi$ per pulse round trip time $T = 2L/\bar{v}_g$ fixes the frequency comb offset. Hence it has been dubbed carrier-envelope (CE) offset frequency.

How precise the condition of vanishing higher-order dispersion is fulfilled in practice could be estimated by knowing that an irregular phase variations between the modes on

the order of 2π are sufficient to completely destroy the stored pulse in the time domain. The phase between adjacent modes of a proper frequency comb advances as $\omega_r t$, *i.e.* typically by some 10^8 times 2π a second. An extra random cycle per second would offset the modes by only 1 Hz from the perfectly regular grid, but destroy the pulse in the same time. Compared to the optical carrier frequency this corresponds to a relative uncertainty of 3 parts in 10^{15} at most, which is already close to the best cesium atomic clocks. Experimentally one observes the same pulse for a much longer time, in some lasers even for months. In fact no deviations have been detected yet at a sensitivity of a few parts in 10^{16} [28, 7, 29, 30].

It should be noted that a more appropriate derivation of the frequency comb must include non-linear shifts of the group and phase velocities because this is used to lock the modes in the first place. In fact it has been shown that initiating the mode-locking mechanism significantly shifts the cavity modes of a laser [31]. Of course the question remains how this mode-locking process forces the cancellation of all pulse deforming dispersive contributions with this precision. Even though this is beyond the scope of this article and details may be found elsewhere [32, 24], the simplest explanation is given in the time domain: Mode locking, *i.e.* synchronizing the longitudinal cavity modes to sum up for a short pulse, is most commonly achieved with the help of the Kerr effect which is expressed in the time domain through

$$(9) \quad n(t) = n_0 + n_2 I(t).$$

Here n_2 denotes a small intensity $I(t)$ dependence of the refractive index $n(t)$. Generally a Kerr coefficient with a fs response time is very small, so that it becomes noticeable only for the high peak intensity of short pulses. Kerr lens mode locking uses this effect in two ways. The radially intensity variation of a Gaussian mode produces a lens that becomes part of the laser resonator for a short pulse. This resonator is designed such that it has larger losses without such a lens, *i.e.* for a superposition of randomly phased modes. In addition self phase modulation can compensate the some de-phasing of the modes. A wave packet that does not deform as it travels because higher-order dispersive terms are compensated by self phase modulation, is called a soliton [33, 34]. The nice feature about this cancellation is that it is self-adjusting: Slightly larger peak intensity extends the pulse duration and reduces the peak intensity leaving the pulse energy constant and vice versa. So that neither the pulse intensity nor the dispersion has to be matched exactly (which would not be possible) to generate a soliton. Of course it helps to pre-compensate higher-order dispersion as good as possible before initiating mode locking. It appears that for the shortest pulses the emission bandwidth is basically given by the bandwidth this pre-compensation is achieved [35, 36]. Once mode locking is initiated, mostly by a mechanical disturbance of the laser cavity, the modes are pulled on the regular grid described by eq. (6). Another way of thinking about this process is that self phase modulation that occurs with the repetition frequency, produces side bands on each mode that will injection lock the neighboring modes by mode pulling. This pulling produces the regular grid of modes and is limited by the injection locking range [37], *i.e.* how well the pre-compensation of higher-order dispersion was done.

2.2. Derivation from the pulse train. – Rather than considering intracavity dispersion, the cavity length and so on, one may simply analyze the emitted pulse train with little consideration how it is generated. For this one assumes that the electric field $E(t)$, measured for example at the output coupling mirror, can be written as the product of a

periodic envelope function $A(t)$ and a carrier wave $C(t)$:

$$(10) \quad E(t) = A(t)C(t) + \text{c.c.}$$

The envelope function defines the pulse repetition time $T = 2\pi/\omega_r$ by demanding $A(t) = A(t - T)$. The only thing about dispersion that should be added for this description, is that there might be a difference between the group velocity and the phase velocity inside the laser cavity. This will shift the carrier with respect to the envelope by a certain amount after each round trip. The electric field is therefore in general not periodic with T . To obtain the spectrum of $E(t)$ the Fourier integral has to be calculated:

$$(11) \quad \tilde{E}(\omega) = \int_{-\infty}^{+\infty} E(t)e^{i\omega t} dt.$$

Separate Fourier transforms of $A(t)$ and $C(t)$ are given by

$$(12) \quad \tilde{A}(\omega) = \sum_{n=-\infty}^{+\infty} \delta(\omega - n\omega_r) \tilde{A}_n \quad \text{and} \quad \tilde{C}(\omega) = \int_{-\infty}^{+\infty} C(t)e^{i\omega t} dt.$$

A periodic frequency chirp imposed on the pulses is accounted for by allowing a complex envelope function $A(t)$. Thus the ‘‘carrier’’ $C(t)$ is defined to be whatever part of the electric field that is non-periodic with T . The convolution theorem allows us to calculate the Fourier transform of $E(t)$ from $\tilde{A}(\omega)$ and $\tilde{C}(\omega)$:

$$(13) \quad \tilde{E}(\omega) = \frac{1}{2\pi} \int_{-\infty}^{+\infty} \tilde{A}(\omega')\tilde{C}(\omega - \omega')d\omega' + \text{c.c.} = \frac{1}{2\pi} \sum_{n=-\infty}^{+\infty} \tilde{A}_n \tilde{C}(\omega - n\omega_r) + \text{c.c.}$$

The sum represents a periodic spectrum in frequency space. If the spectral width of the carrier wave $\Delta\omega_c$ is much smaller than the mode separation ω_r , it represents a regularly spaced comb of laser modes just like eq. (6), with identical spectral line shapes, namely the line shape of $\tilde{C}(\omega)$ (see fig. 1). If $\tilde{C}(\omega)$ is centered at say ω_c , then the comb is shifted from containing only exact harmonics of ω_r by ω_c . The center frequencies of the mode members are calculated from the mode number n [3, 8, 25, 26]:

$$(14) \quad \omega_n = n\omega_r + \omega_c.$$

The measurement of the frequency offset ω_c [2-8]. as described below usually yields a value modulo ω_r , so that renumbering the modes will restrict the offset frequency to smaller values than the repetition frequency and again yields eq. (6).

The individual modes can be separated with a suitable spectrometer if the spectral width of the carrier function is narrower than the mode separation: $\Delta\omega_c \ll \omega_r$. This condition is easy to satisfy, even with a free-running titanium-sapphire laser. If a single mode is selected from the frequency comb, one obtains a continuous wave. However it is easy to show that a grating with sufficient resolution would be at least as large as the laser cavity, which appears unrealistic for a typical laser with a 2 m cavity length. Fortunately for experiments performed so far it has never been necessary to resolve a single mode in the optical domain as explained in sect. 3.

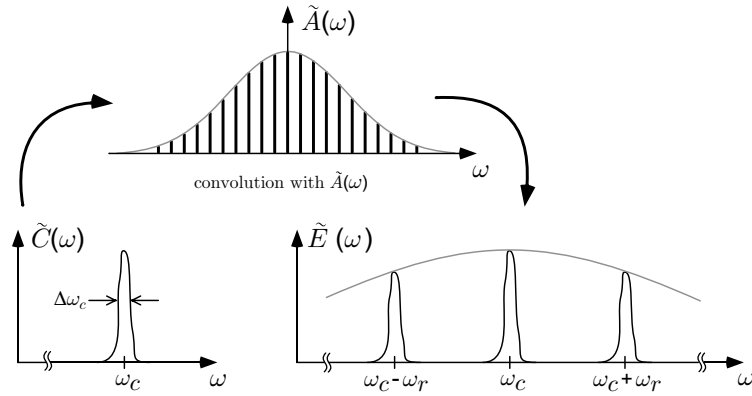


Fig. 1. – The spectral shape of the carrier function (left), assumed to be narrower than the pulse repetition frequency ($\Delta\omega_c \ll \omega_r$), and the resulting spectrum according to eq. (13) after modulation by the envelope function (right).

Now let us consider two instructive examples of possible carrier functions. If the carrier wave is monochromatic $C(t) = e^{-i\omega_c t - i\varphi}$, its spectrum will be δ -shaped and centered at the carrier frequency ω_c . The individual modes are also δ -functions $\tilde{C}(\omega) = \delta(\omega - \omega_c)e^{-i\varphi}$. The frequency offset (14) is identified with the carrier frequency. According to eq. (10) each round trip will shift the carrier wave with respect to the envelope by $\Delta\varphi = \arg(C(t - T)) - \arg(C(t)) = \omega_c T$ so that the frequency offset is given

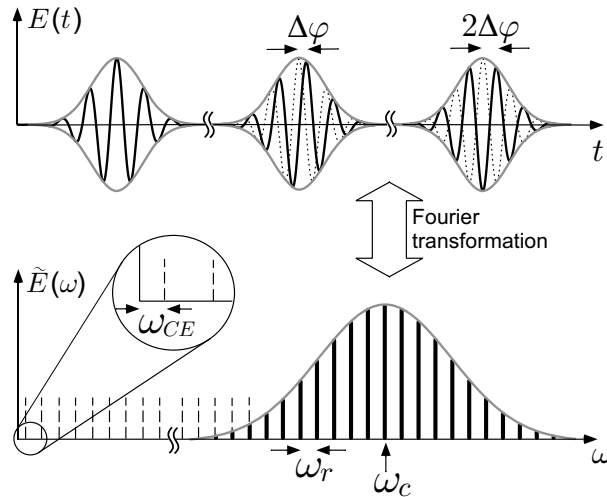


Fig. 2. – Consecutive un-chirped pulses ($A(t)$ real) with carrier frequency ω_c and the corresponding spectrum (not to scale). Because the carrier propagates with a different velocity within the laser cavity than the envelope (phase- and group velocity), the electric field does not repeat itself after one round trip. A pulse-to-pulse phase shift $\Delta\varphi$ results in an offset frequency of $\omega_{CE} = \Delta\varphi/T$. The mode spacing is given by the repetition rate ω_r . The width of the spectral envelope is given by the inverse pulse duration up to a factor order unity that depends on the pulse shape (the time bandwidth product of a Gaussian pulse for example is 0.441 [24]).

by $\omega_{\text{CE}} = \Delta\varphi/T$ [3, 8, 25, 26]. In a typical laser cavity this pulse-to-pulse carrier-envelope phase shift is much larger than 2π , but measurements usually yield a value modulo 2π . The restriction $0 \leq \Delta\varphi \leq 2\pi$ is synonymous with the restriction $0 \leq \omega_{\text{CE}} \leq \omega_r$ introduced earlier. Figure 2 sketches this situation in the time domain for a chirp free-pulse train.

As a second example consider a train of half-cycle pulses like

$$(15) \quad E(t) = E_0 \sum_k e^{-\left(\frac{t-kT}{\tau}\right)^2}.$$

In this case the electric field would be repetitive with the round trip time. Therefore $C(t)$ is a constant and its Fourier transform is a delta-function centered as $\omega_c = 0$. If it becomes possible to build a laser able to produce a stable pulse train of that kind, all the comb frequencies would become exact harmonics of the pulse repetition rate. Obviously, this would be an ideal situation for optical frequency metrology⁽³⁾.

As these examples are instructive it is important to note that one neither relies on assuming a strictly periodic electric field nor that the pulses are unchirped. The strict periodicity of the spectrum as stated in eq. (13), and the possibility to generate beat notes between continuous lasers and single modes [38], are the only requirement that enables precise optical to radio frequency conversions.

In a real laser the carrier wave will not be a clean sine wave as in the above example. The mere periodicity of the field, allowing a pulse-to-pulse carrier envelope phase shift, already guarantees the comb-like spectrum. Very few effects can disturb that property. In particular, for an operational frequency comb, both ω_r and ω_{CE} will be servo controlled so that slow drifts are compensated. The property that the comb method really relies on, is the mode spacing being constant across the spectrum. As explained above, even a small deviation from this condition will have very quick and devastating effects on the pulse envelope. Not even an indefinitely increasing chirp could disturb the mode spacing constancy, as this can be seen as a constantly drifting carrier frequency that does not perturb the spectral periodicity but shifts the comb as a whole. However, the phase of individual modes can fluctuate about an average value required for staying in lock with the rest of the comb. This will cause noise that can broaden individual modes as discussed in the next section.

2.3. Linewidth of a single mode. – The modes of a frequency comb have to be understood as continuous laser modes. As such they possess a linewidth which is of interest here. Of course as usual in such a case, several limiting factors are effective at the same time. It is instructive to derive the Fourier limited linewidth that is due to observing the pulse train for a limited number of pulses only. Following a derivation by Siegman [37]⁽⁴⁾ the linewidth of a train of N pulses can be derived. In accordance with the previous section we assume that the pulse train consists of identical pulses $\mathcal{E}(t)$ separated in time by T and subjected to a pulse-to-pulse phase shift of $e^{i\Delta\varphi}$:

$$(16) \quad E(t) = \frac{E_0}{\sqrt{N}} \sum_{m=0}^{N-1} e^{im\Delta\varphi} \mathcal{E}(t - mT).$$

⁽³⁾ It should be noted though that this is a rather academic example because such a pulse would be deformed quickly upon propagation since it contains vastly distinct frequency components with different diffraction. For example, the DC component that this carrier certainly has, would not propagate at all.

⁽⁴⁾ The carrier envelope phase shift was ignored in [37] but can easily be accounted for here.

For decent pulse shapes, that fall off at least as $\propto 1/t$ from the maximum, this series converges even as N goes to infinity. Using the shift theorem

$$(17) \quad \mathcal{FT} \{ \mathcal{E}(t - \tau) \} = e^{-i\omega\tau} \mathcal{FT} \{ \mathcal{E}(t) \}$$

one can relate the Fourier transform of the pulse train $E(t)$ to the Fourier transform of a single pulse $\tilde{\mathcal{E}}(\omega)$. With the sum formula for the geometric series this becomes

$$(18) \quad \tilde{E}(\omega) = \frac{E_0 \tilde{\mathcal{E}}(\omega)}{\sqrt{N}} \sum_{m=0}^{N-1} e^{-im(\omega T - \Delta\varphi)} = \frac{E_0 \tilde{\mathcal{E}}(\omega)}{\sqrt{N}} \frac{1 - e^{-iN(\omega T - \Delta\varphi)}}{1 - e^{-i(\omega T - \Delta\varphi)}}.$$

Now the intensity spectrum for N pulses $I_N(\omega)$ may be calculated from the spectrum of a single pulse $I(\omega) \propto |\tilde{\mathcal{E}}(\omega)|^2$:

$$(19) \quad I_N(\omega) = \frac{1 - \cos(N(\omega T - \Delta\varphi))}{N(1 - \cos(\omega T - \Delta\varphi))} I(\omega).$$

Figure 3 sketches this result for several N . As the spectrum of single pulse is truly a continuum, the modes are emerging and becoming sharper as more pulses are added. This is similar to the diffraction from a grating that becomes sharper as more grating lines are illuminated. The spectral width of a single mode can now be calculated from (19) and may be approximated by $\Delta\omega \approx \sqrt{24}/TN$ for the pulse train observation time NT . From this the Fourier limited line width is reduced after one second of observation time NT to $\sqrt{24}/2\pi \text{ Hz} \approx 0.78 \text{ Hz}$ and further decreases as the inverse observation time. In the limit of an infinite number of pulses pulse the spectral shape of the modes approximate delta-functions with $x = \omega T - \Delta\varphi \approx 2\pi n$

$$(20) \quad \frac{1}{2\pi} \lim_{N \rightarrow \infty} \frac{1 - \cos(Nx)}{N(1 - \cos(x))} \approx \frac{1}{\pi} \lim_{N \rightarrow \infty} \frac{1 - \cos(Nx)}{Nx^2} = \delta(x).$$

The whole frequency comb becomes an equidistant array of delta-functions:

$$(21) \quad I_N(\omega) \rightarrow I(\omega) \sum_n \delta(\omega T - \Delta\varphi - 2\pi n).$$

The Fourier limit to the linewidth derived here is important when only a number of pulses can be used for example for direct comb spectroscopy as will be discussed in subsect. 4'5. On the other hand, when a large number of pulses contribute to the signal, for example when measuring the carrier envelope beat note, other limits enter. In most of these cases acoustic vibrations seem to set the limit as can be seen by observing that the noise of the repetition rate of an unstabilized laser dies off very steeply for frequencies above typical ambient acoustic vibrations around 1 kHz [39]. Even if these fluctuations are controlled as they can be with the best continuous wave lasers, a limit set by quantum mechanics in terms of the power-dependent Schawlow-Townes formula applies. Remarkably the total power of *all* modes enters this formula to determine the line width of a *single* mode [40]. In fact subhertz linewidths have been measured across the entire frequency comb when it is stabilized appropriately [41, 42].

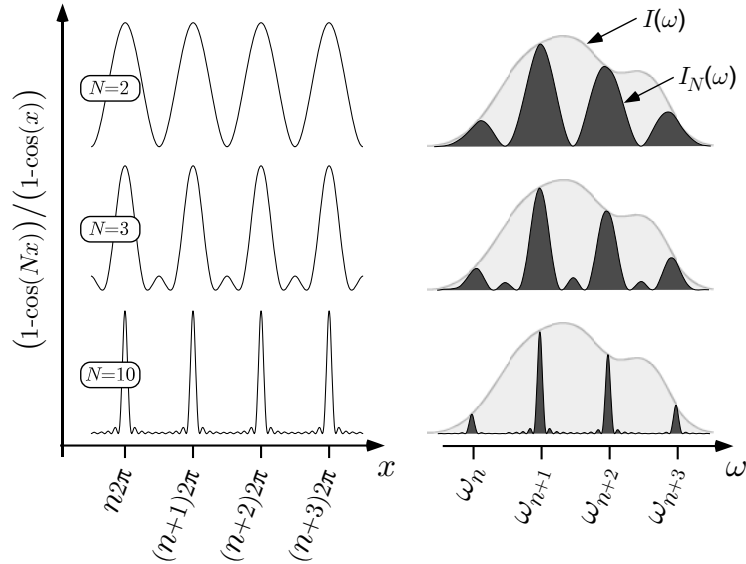


Fig. 3. – Left: The function $(1 - \cos(Nx))/(1 - \cos(x))$ normalized to the peak for $N = 2, 3$ and 10 pulses. The maxima are at $x = \omega_n T - \Delta\varphi = 2\pi n$ with integer n . From that and redefining $\omega_r = 2\pi/T$ and $\omega_{CE} = \Delta\varphi/T$ we derive again the frequency comb equation (6). Right: The resulting frequency comb spectrum is given by the spectrum of a single pulse multiplied with the comb function at the left-hand side.

2.4. Generating an octave spanning comb. – The spectral width of a pulse train emitted by a fs laser can be significantly broadened in a single-mode fiber [34] by self-phase modulation. According to eq. (9) assuming a single-mode carrier wave, a pulse that has propagated the length l acquires a self-induced phase shift of

$$(22) \quad \Phi_{NL}(t) = -n_2 I(t) \omega_c l / c \quad \text{with} \quad I(t) = \frac{1}{2} c \epsilon_0 |A(t)|^2 .$$

For fused silica the non-linear coefficient is comparatively small but almost instantaneous even on the time scale of fs pulses. This means that different parts of the pulse travel at different speed. The result is a frequency chirp across the pulse without affecting its duration. The pulse is no longer at the Fourier limit so that the spectrum is much broader than the inverse pulse duration where the extra frequencies are determined by the time derivative of the self-induced phase shift $\dot{\Phi}_{NL}(t)$. Self-phase modulation modifies the envelope function in eq. (10) according to

$$(23) \quad A(t) \longrightarrow A(t) e^{i\Phi_{NL}(t)} .$$

Because $\Phi_{\text{NL}}(t)$ has the same periodicity as $A(t)$ the comb structure of the spectrum is maintained and the derivations of subsect. 2.2 remain valid because periodicity of $A(t)$ was the only assumption made. An optical fiber is most appropriate for this process because it can maintain the necessary small focus area over a virtually unlimited length. In practice, however, other pulse reshaping mechanisms, both linear and non-linear, are present so that the above explanation is too simple.

Higher-order dispersion is usually limiting the effectiveness of self-phase modulation as it increases the pulse duration and therefore lowers the peak intensity after a propagation length of a few mm or cm for fs pulses. One can get a better picture if pulse broadening due to group velocity dispersion $k''(\omega_c)$ is included. To measure the relative importance of the two processes, the dispersion length L_D (the length that broadens the pulse by a factor $\sqrt{2}$) and the non-linear length L_{NL} (the length that corresponds to the peak phase shift $\Phi_{\text{NL}}(t=0) = 1$) are used [34]:

$$(24) \quad L_D = \frac{4 \ln(2) \tau^2}{|k''(\omega_c)|} \quad L_{\text{NL}} = \frac{c A_f}{n_2 \omega_c P_0},$$

where τ_0 , A_f and $P_0 = (1/2)A_f c \varepsilon_0 |A(t=0)|^2$ are the initial pulse duration, the effective fiber core area and the pulse peak power. In the dispersion dominant regime $L_D \ll L_{\text{NL}}$ the pulses will disperse before any significant non-linear interaction can take place. For $L_D > L_{\text{NL}}$ spectral broadening could be thought as effectively taking place for a length L_D even though the details are more involved. The total non-linear phase shift can therefore be approximated by the number of non-linear lengths within one dispersion length. As this phase shift occurs roughly within one pulse duration τ , the spectral broadening is estimated to be $\Delta\omega_{\text{NL}} = L_{\text{NL}}/L_D \tau$. As an example consider a silica single mode fiber (Newport F-SF) with $A_f = 26 \mu\text{m}^2$, $k''(\omega_c) = 281 \text{ fs/cm}^2$ and $n_2 = 3.2 \times 10^{-16} \text{ cm}^2/\text{W}$ that is seeded with $\tau = 73 \text{ fs}$ Gaussian pulses (FWHM intensity) at 905 nm with 225 mW average power and a repetition rate of 76 MHz [3, 4]. In this case the dispersion length becomes 6.1 cm and the non-linear length 35 mm. The expected spectral broadening of $L_{\text{NL}}/L_D \tau = 2\pi \times 44 \text{ THz}$ is indeed very close to the observed value [3].

It turns out that within this model the spectral broadening is independent of the pulse duration τ because $P_0 \propto \tau$. Therefore using shorter pulses may not be effective for extending the spectral bandwidth beyond an optical octave as required for simple self-referencing (see sect. 3). However, very efficient spectral broadening can be obtained in microstructure fiber⁽⁵⁾ that can be manufactured with $k''(\omega_c) \approx 0$ around a design wavelength [43-45]. In this case the pulses are broadened by other processes (linear and non-linear) than group velocity dispersion as they propagate along the fiber. Eventually this will also terminate self-phase modulation and the dispersive length has to be replaced appropriately in the above analysis. At this point a whole set of effects enter such as Raman and Brillouin scattering, optical wave breaking and modulation instability [34]. Some of these processes even spoil the usefulness of the broadened frequency combs as they amplify noise.

A microstructure fiber uses an array of submicron-sized air holes that surround the

⁽⁵⁾ Some authors refer to these fibers as photonic crystal fibers that need to be distinguished from photonic bandgap fibers. The latter use Bragg diffraction to guide the light, while the fibers discussed here use the traditional index step, with the refractive index determined by the air filling factor.

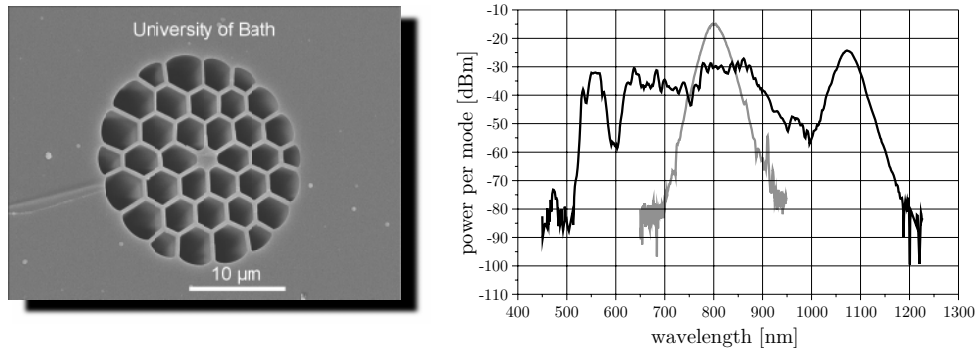


Fig. 4. – Left: SEM image of a the core of a microstructure fiber made at the University of Bath, UK [43]. The light is guided in the central part but the evanescent part of the wave penetrates into the air holes that run parallel to the fiber core and lower the effective refractive index without any doping. The guiding mechanism is the same as in a conventional single mode fiber. Right: Power per mode on a logarithmic scale (0 dBm = 1 mW). The lighter 30 nm (14 THz–3 dB) wide spectrum displays the laser intensity and the darker octave spanning spectrum (532 nm through 1064 nm) is observed after the microstructure fiber that was 30 cm long. The laser was operated at $\omega_r = 2\pi \times 750$ MHz (modes not resolved) with 25 fs pulse duration. An average power of 180 mW was coupled through the microstructure fiber [47].

fiber core and run the length of a silica fiber to obtain a desired effective dispersion. This can be used to maintain the high peak power over an extended propagation length and to significantly increase the spectral broadening. With these fibers it became possible to broaden low peak power, high repetition rate lasers to beyond one optical octave as fig. 4 shows.

A variant of the microstructure fibers are regular single-mode fibers that have been pulled in a flame to form a tapered section of a few cm lengths [46]. When the diameter of the taper becomes comparable to the core diameter of the microstructure fibers, pretty much the same properties are observed. In the tapered section the action of the fiber core is taken over by the whole fiber. The original fiber core then is much too small to have any influence on the light propagation. The fraction of evanescent field around the taper and along with it the dispersion characteristics can be adjusted by choosing a suitable taper diameter.

The peak intensity that can be reached with a given mode-locked laser does not only depend on the pulse duration but critically on the repetition rate. Because most laser have pretty much the same average output power, a lower repetition rate concentrates this available power into fewer pulses per second. Comparing different laser systems the repetition rates in use cover more than 12 orders of magnitude from the most powerful lasers (one laser shot per 1000 s) to highly repetitive lasers at $\omega_r = 2\pi \times 2$ GHz [48]. It has been long known that with enough peak intensity one can produce very wide spectra that were initially called “white light continuum”. Unfortunately for a long time this was only possible at a repetition rate of around 1 kHz that indeed justifies the name: The generated spectrum could be called a “continuum” as there was not much hope to resolve the modes in any way for self-referencing or by a beat note with another cw laser. Because of its high efficiency the microstructure fiber allowed to generate an octave wide spectra with repetition rates up to 1 GHz that conveniently allowed the beat notes to be

separated as described in sect. 3. In addition a large mode spacing puts more power in each mode improving the signal to noise of the beat notes.

The laser that quickly became the working horse in the field for this reason was a rather compact titanium-sapphire ring laser with typical repetition rates of 500 MHz to 1 GHz [48]. The ring design solved another problem that is frequently encountered when coupling a laser into an optical fiber. Optical feedback from the fiber may disturb the laser operation and even prevent mode locking in some cases. The standard solution to this problem would be to place an optical isolator between the fiber and the laser. In this case however such a device would have almost certainly enough group velocity dispersion to prevent any subsequent spectral broadening if this is not compensated for. In a ring laser the pulses reflected back from the fiber travel in the opposite direction and do not talk to the laser pulses unless they meet inside the laser crystal. The latter can be prevented by observing the distance of the fiber from the laser. A disadvantage of these lasers is that they are not easy to align and have so far not become turn key systems that can be operated unattended for a long time say in an all optical atomic clock (see below).

Even though microstructure fibers have allowed the simple $f - 2f$ self-referencing for the first time, they also have some drawbacks. To achieve the desired properties, the microstructure fibers need to have a rather tiny core. The coupling to this core causes problems due to mechanical instabilities and temperature drifts even with low level and stable mounts. Another problem is the observed but not fully understood strong polarization dependence of the fibers broadening action. The possibility of long-term continuous operation is not so much of an issue for spectroscopy, because data taking in these experiments usually do not last very long and they need some attention on their own. However, this possibility seem to be a key requirement operating an all optical atomic clock. So far the only way to operate such a system unattended for hours was to use a set of additional servo systems that continuously measure and correct deviations from the fiber coupling and polarization [49].

Another problem with spectral broadening by self phase modulation in general is a excess noise level of the beat notes well above the shot noise limit [50, 51]. In fact using the 73 fs laser mentioned above with a microstructure fiber, a two-octave-spanning spectrum is generated within a few centimeters of fiber. However this spectrum does not separate into modes that could be detected by a beat note measurement with a cw laser but consist of noise [52]. One possible explanation is the Raman effect that produces strong gain about 13 THz to the red from the pump wavelength. If this gain is not seeded, it may trigger an avalanche of photons from the vacuum, that bear no phase relationship to the carrier wave and coherence is lost⁽⁶⁾. For sufficiently broad input spectra the Raman gain is seeded coherently with modes from the frequency comb amplifying the low-frequency modes at the cost of the high-frequency modes. For longer pulses, say below $0.441/(13 \text{ THz}) = 34 \text{ fs}$ for Gaussian pulse shape, less seeding occurs. In fact a more detailed calculation predicts that enough coherence is maintained by self-phase modulation if the seeding the pulses are shorter than 50 fs [53].

By going to shorter pulses for the the seed laser this problem can be handled but the alignment issue remains. On the other hand, lasers that reach an octave-spanning

⁽⁶⁾ This process is called “stimulated Raman scattering” because all but the first photon is produced by stimulated emission. It should be noted though that the first spontaneous photon destroys the coherence of the whole process.

spectrum without using any external self-phase modulation can solve this problem [54-57]. So far however, these lasers seem to be rather delicate to handle so that one alignment problem is replaced with another. An interesting alternative are lasers that avoid the use of microstructure fibers in another way. For wide-band but not quite octave-spanning lasers, a $2f - 3f$ self-referencing becomes possible by doubling the blue wing of the spectrum and beat it with the tripled red wing [58,59]. Such a system can remain phase locked unattended for several hours without the burden of having extra servo systems. Related but somewhat simpler seems to be a laser that produces pulses short enough so that a little bit of self-phase modulation generated in single pass through a difference frequency generating crystal provides sufficient spectral broadening [60].

Yet another class of frequency combs that can stay in lock for even longer times are fs fiber lasers [61]. The most common type is the erbium-doped fiber laser that emits within the telecom band around 1500 nm. For this reason advanced and cheap optical components are available to build such a laser. The mode-locking mechanism is similar to the Kerr lens method, except that non-linear polarization rotation is used to favor the pulsed high peak intensity operation. Up to a short free-space section that can be build very stable, these lasers have no adjustable parts. Bulk fused silica has its zero group velocity dispersion at around $1.2 \mu\text{m}$ but this can be shifted to $1.5 \mu\text{m}$ in an optical fiber. If, in addition, the radial dependence of the refractive index is designed to obtain a small core area A_f , the fiber becomes what is called a highly non-linear fiber (HNLF) without any microstructure. These HNLF's are commercially available and can be spliced directly to a fs fiber laser. This virtually eliminates the remaining alignment sensitive parts as the free space frequency doubling stage and beat note detection can be build rather robust. Continuous stabilized operation for many hours [62,63] have been reported. The Max-Planck Institute für Quantenoptik in Garching/Germany operates a fiber based self-referenced frequency comb that stays locked without interruption for months. A significantly large jitter of the observed CE-beat note has been observed in these lasers and can either be suppressed by using low noise pump lasers [64] or eliminated with a fast servo system.

3. – Self-referencing

The measurement of ω_{CE} fixes the position of the whole frequency comb and is called self-referencing. The method relies on measuring the frequency gap between *different* harmonics derived from the *same* laser or frequency comb. The first crude demonstration [2] employed the 4th and the 3.5th harmonic of a $f = 88.4 \text{ THz}$ ($3.39 \mu\text{m}$) laser to determine ω_{CE} according to $4\omega_n - 3.5\omega_{n'} = (4n - 3.5n')\omega_r + 0.5\omega_{\text{CE}} = 0.5\omega_{\text{CE}}$ with $4n - 3.5n' = 0$. To achieve the condition of the latter equation, both n and n' have to be active modes of the frequency comb. The required bandwidth is $0.5f = 44.2 \text{ THz}$ which is what the 73 fs laser together with a single-mode fiber as discussed in the previous section can generate.

A much simpler approach is to fix the absolute position of the frequency comb by measuring the gap between ω_n and ω_{2n} of modes taken directly from the frequency comb [4-8]. In this case the carrier-envelope offset frequency ω_{CE} is directly produced by beating the frequency doubled⁽⁷⁾ red wing of the comb $2\omega_n$ with the blue side of the

⁽⁷⁾ It should be noted that this does not simply mean the doubling of each individual mode, but the general sum frequencies generation of all modes. Otherwise the mode spacing, and therefore

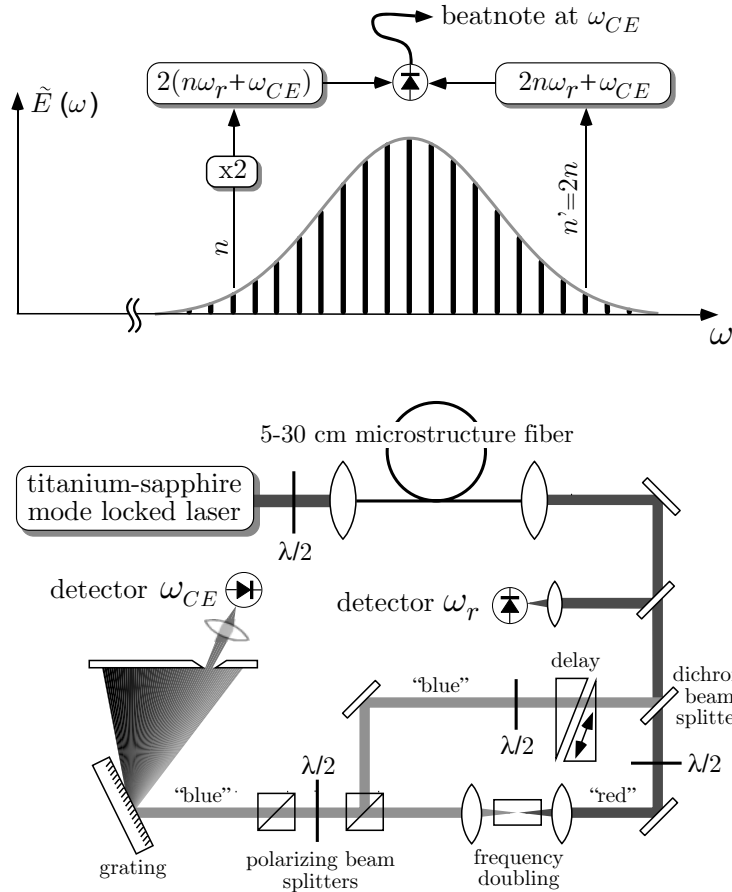


Fig. 5. – Top: $f - 2f$ self-referencing by detecting a beat note at ω_{CE} between the frequency doubled “red” wing $2(n\omega_r + \omega_{CE})$ of the frequency comb and the “blue” modes at $2n\omega_r + \omega_{CE}$. Bottom: Layout of the self-referencing scheme. See text for details.

comb at ω_{2n} : $2\omega_n - \omega_{n'} = (2n - n')\omega_r + \omega_{CE} = \omega_{CE}$ where again the mode numbers n and n' are chosen such that $(2n - n') = 0$. This approach requires an octave spanning comb, *i.e.* a bandwidth of 375 THz if centered at the titanium-sapphire gain maximum at 800 nm.

Figure 5 sketches the $f - 2f$ self-referencing method. The spectrum of a titanium-sapphire mode-locked laser is first broadened to more than one optical octave with a microstructure fiber. A broad-band $\lambda/2$ wave plate allows to choose the polarization with the most efficient spectral broadening. After the fiber a dichroic mirror separates the infrared (“red”) part from the green (“blue”). The former is frequency doubled in a non-linear crystal and reunited with the green part to create a wealth of beat notes, all at ω_{CE} . These beat notes emerge as frequency difference between $2\omega_n - \omega_{2n}$ according to

the repetition rate, would be doubled as well.

eq. (6) for various values of n . The number of contributing modes is given by the phase matching bandwidth $\Delta\nu_{pm}$ of the doubling crystal and can easily exceed 1 THz. To bring all these beat notes at ω_{CE} in phase, so that they all add constructively an adjustable delay in form of a pair of glass wedges or corner cubes is used. It is straightforward to show that the condition for a common phase of all these beat notes is that the green and the doubled infrared pulse reach the photo detector at the same time. The adjustable delay allows to compensate for different group delays, including the fiber. In practice the delay needs to be correct within $c\Delta\nu_{pm}$ which is $300\ \mu\text{m}$ for $\Delta\nu_{pm} = 1\ \text{THz}$. Outside this range a beat note at ω_{CE} is usually not detectable.

Whereas the half wave plates in the two interferometer arms are used to adjust for whatever polarization exits the microstructure fiber, the half wave plate between the two polarizing beam splitters helps to find the optimum relative intensity of the two beating pulses. It can be shown that the maximum signal to noise ratio is obtained for equal intensities reaching the detector within the optical bandwidth that contributes to the beat note [3]. In practice this condition is most conveniently adjusted by observing the signal-to-noise ratio of the ω_{CE} beat note with a radio frequency spectrum analyzer. For this purpose a low-cost analog device that operates up to ω_r is usually sufficient.

A grating is used to prevent the extra optical power, that does not contribute to the signal but adds to the noise level, from reaching the detector. Typically only a large relative bandwidth of say $1\ \text{THz}/375\ \text{THz}$ needs to be selected so that a very moderate resolution illuminating 375 lines is sufficient. For this reason it is usually not necessary to use a slit between the grating and the photo detector. Sufficient resolution can be reached with a small low-cost 1200 lines per mm grating illuminated with a beam collimated with $\times 10$ microscope objective out of the microstructured fiber.

When detecting the beat note as described above, more than one frequency component is obtained for two reasons. First of all any beat note, even between two cw lasers, generates two components because the radio frequency domain cannot decide which of the two optical frequencies is larger than the other. Secondly, observing the beat notes between frequency combs, not only the desired component $k = 2n - n' = 0$ is registered, but all integer values of k , positive and negative contribute, up to the bandwidth of the photo detector. This leads to a set of radio frequency beat notes at $k\omega_r \pm \omega_{CE}$ for $k = \dots - 1, 0, +1 \dots$. In addition the repetition rate, including its harmonics will most likely give the strongest components. After carefully adjusting the nonlinear interferometer, spatially and spectrally, and scanning the delay line for the proper pulse arrival times, the radio frequency spectrum may look like the one shown in fig. 6. A low-pass filter with a cut-off frequency of $0.5\omega_r$ selects exactly one beat note at $\pm\omega_{CE}$. The design of such a filter may be tricky, mostly depending on how much stronger the repetition rate signal exceeds the beat note at ω_{CE} . The sketch in fig. 6 gives a feeling on how steep this filter needs to be at the cut-off in order to suppress the unwanted components below the noise level. Such a suppression is required for taking the full advantage of the signal-to-noise ratio. For this reason it is desirable to work at higher repetition rates. At ω_r around $2\pi \times 800\ \text{MHz}$, as used mostly for the ring titanium-sapphire lasers described above, the filter requirements are much more relaxed than say at 80 MHz. In addition, a larger repetition rate concentrates more power in each mode further improving the beat notes with the frequency comb. It should be noted though, that currently higher repetition rates cannot be used because the associated lower peak power will make it difficult to achieve spectral broadening beyond one optical octave as detailed in subsect. 2'4.

As described, both degrees of freedom ω_r and ω_{CE} of the frequency comb can be measured up to a sign in ω_{CE} that will be discussed below. For stabilization of these

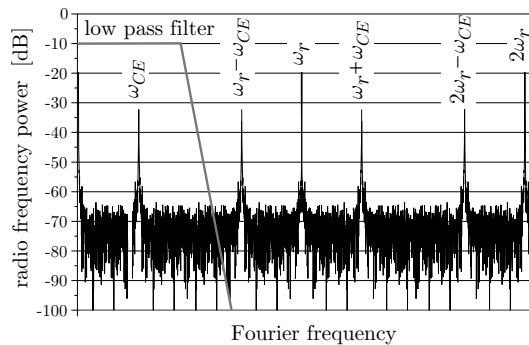


Fig. 6. – Radio frequency spectrum produced by a self-referencing non-linear interferometer such as the $f - 2f$ interferometer shown in fig. 5. A low-pass filter with a cut-off at $0.5\omega_r$ selects the component at $\pm\omega_{CE}$.

frequencies, say relative to a radio frequency reference, it is necessary to be able to control them. Again the repetition rate turns out to be simpler. By mounting one of the lasers cavity mirrors on a piezo electric transducer allows to control the pulse round trip time. Another option is offered by mode-locked lasers that use prism pairs to compensate the intracavity group velocity dispersion. In this case tipping the mirror at the dispersive end where the cavity modes are spatially separated, changes the relative cavity lengths of the individual modes and thereby the mode spacing in frequency space [7]. In practice the detected repetition frequency is mixed with the radio frequency reference, *i.e.* the frequency difference is generated, low-pass filtered and with appropriate gain send back to the piezo electric transducer. When properly designed such a phase-locked loop forces one oscillator, the repetition rate, to stay in phase with another, the radio frequency reference. Because these servo systems are standard components in many electronic devices such as FM radio receivers, a large amount of literature exists on their design and stability analysis [65].

Setting up a phase-locked loop for the repetition rate therefore seems rather straightforward. However, some caution concerning the servo bandwidth needs to be observed. It turns out that the large frequency multiplication factor n in eq. (6) may also multiplies the noise of the reference oscillator. The phase noise power for direct frequency multiplication by n increases proportional to n^2 [66], so that a factor of $n = 10^6$, that would take us from a 100 MHz radio frequency signal to a 100 THz optical signal, increases the noise by 120 dB. On this basis it has been predicted that, using even the best available reference oscillator, it is impossible to multiply in a single step from the radio frequency domain into the optical [67]. The frequency comb does just that but avoids the predicted carrier collapse. In this case the laser acts as a flywheel in the optical that does not follow the fast phase fluctuations of the reference oscillator but averages them out. In this sense the n^2 multiplication law does not apply, because it assumes a phase stiff frequency multiplication that would correspond to an infinite servo bandwidth. Fortunately a typical free-running titanium-sapphire mode-locked laser shows very good phase stability of the pulse train on its own. For averaging times shorter than typical acoustic vibrations of several ms period, such a laser shows better phase stability than a high-quality synthesizer. It is therefore essential to use a moderate servo bandwidth for phase

locking the repetition rate of a few 100 Hz at most. A small servo bandwidth may be implemented electronically by appropriate filtering or mechanically by using larger masses than the usual tiny mirrors mounted on piezo transducers for high servo speed. In some case a complete one inch mirror mount has been moved for controlling the repetition rate [15].

Controlling the carrier envelope frequency requires some effort. Experimentally it turned out that the energy of the pulse stored inside the mode locked laser has a strong influence on ω_{CE} . After initial explanations of this effects turned out to be too crude, more appropriate mechanisms have been found [68,69]. Conventional soliton theory [33] predicts a dependence of the phase velocity but no dependence of the group velocity on the pulse peak intensity. Any difference in the cavity round trip phase delay and the cavity round trip group delay results in a pulse to pulse carrier envelope phase shift and therefore a non-vanishing ω_{CE} . However, the intensity dependence of that effect may turn out to have the wrong sign [70]. The reason is that higher-order effects, usually neglected in the conventional soliton theory, play an important role. The Raman effect in the titanium-sapphire crystal produces an intensity-dependent redshift that in turn affects the group round trip time. In general this leads to an extra term in eq. (8) for the pulse to pulse carrier envelope phase shift per round trip [69]:

$$(25) \quad \Delta\varphi = \omega_c \left(\frac{2L}{\bar{v}_g} - \frac{2L}{\bar{v}_p} + BI_p \right).$$

Because this phase shift is directly proportional to ω_{CE} this equation also describes its dependence on the pulse peak power I_p . The magnitude of the parameter B may best be determined experimentally, as it turns out to depend on the operating parameters of the mode-locked laser. In some cases it even changes in sign as the pump laser intensity is changed [51].

To phase lock the carrier envelope offset frequency ω_{CE} , one uses an actuator, in most cases an acousto-optic modulator, that drains an adjustable part of the pump laser power. Electro-optic modulators have also been used, but they have the disadvantage that they need to a bias voltage that wastes some of the pump energy to work in the linear regime. To servo control the phase of the ω_{CE} component usually requires much more servo bandwidth than locking the repetition rate. How much is needed in practice depends on the type of laser, the intensity and beam pointing stability of the pump laser and the phase detector in use. Mode-locked lasers that use pairs of prisms to compensate for group velocity dispersion generally show a much larger carrier envelope frequency noise. This is because intensity fluctuations slightly change the pulse round trip path because of the intensity-dependent refraction of the titanium-sapphire crystal [71]. Even small variations of the beam pointing result in a varying prism intersection. It should be noted that already 50 μm of extra BK7 glass in the path, shifts the carrier envelope phase by 2π and the carrier envelope frequency by ω_r . In most cases the carrier envelope frequency fluctuations seem to be dominated by the pump laser noise, so that stabilizing ω_{CE} with a modulator as described above even reduces this noise. Today titanium-sapphire lasers are mostly pumped by frequency doubled solid-state lasers that seem to show some differences between the models currently on the market [72]. Fiber-based mode-locked lasers used to have significantly larger noise in the carrier envelope beat note than titanium-sapphire lasers before the semiconductor pump lasers have been stabilized carefully [64].

In most cases a simple mixer is not sufficient to detect the phase of ω_{CE} relative to a reference oscillator as the expected in-loop phase fluctuations are usually much larger as for the ω_r servo. Prescalers or forward-backward counting digital phase detectors may be used to allow for larger phase fluctuations, that in turn allow the use of moderate speed (several 10 kHz) electronics. A complete circuit that has been used for that purpose very successfully is published in [73]. Stabilizing the carrier envelope frequency, even though it generally requires faster electronics, does not have the stability and accuracy issues that enter via the repetition rate due to the large factor n in eq. (6). Any fluctuation or inaccuracy in ω_{CE} just adds to the optical frequencies rather than in the radio frequency domain where it is subsequently multiplied by n .

None of the controls discussed here acts solely on either frequency ω_{CE} and ω_r . In general a linear combination of the two is affected. In practice this turns out to be not important because the different speeds of the two servo systems ensure that they do not influence each other.

Measuring the frequency of an unknown cw laser at ω_L with a stabilized frequency comb, involves the creation of yet another beat note ω_b with the comb. For this purpose the beam of the cw laser is matched with the beam that contains the frequency comb, say with similar optics components as used for creating the carrier envelope beat note. A dichroic beam splitter, just before the grating in fig. 5, could be used to reflect out the spectral region of the frequency comb around ω_L without effecting the beat note at ω_{CE} . This beam would then be fed into another set-up consisting of two polarizing beam splitters, one half wave plate, a grating and a photo detector for an optimum signal-to-noise ratio. The frequency of the cw laser is then given by

$$(26) \quad \omega_L = n\omega_r \pm \omega_{\text{CE}} \pm \omega_b,$$

where the same considerations as above apply for the sign of the beat note ω_b . These signs may be determined by introducing small changes to one of the frequencies with a known sign while observing the sign of changes in another frequency. For example the repetition rate could be increased by picking a slightly different frequency of the reference oscillator. If ω_L stays constant we expect ω_b to decrease (increase) if the “+” sign (“-” sign) is correct.

The last quantity that needs to be determined is the mode number n . If the optical frequency ω_L is already known to a precision better than the mode spacing, the mode number can simply be determined by solving the corresponding equation (26) for n and allowing for an integer solution only. A coarse measurement could be provided by a wave meter for example if its resolution and accuracy is trusted to be better than the mode spacing of the frequency comb. If this is not possible, at least two measurements of ω_L with two different and properly chosen repetition rates may leave only one physically meaningful value for ω_L [27].

4. – Scientific applications

In this section a few experiments in fundamental research where optical frequency measurements have been applied are discussed. Before the introduction of optical frequency combs only a few measurements of visible light could be carried out. Since then not only the available data has multiplied but also its accuracy has improved significantly. Maybe even more important, the frequency combs have enabled the construction of all optical atomic clocks that are treated in sect. 5.

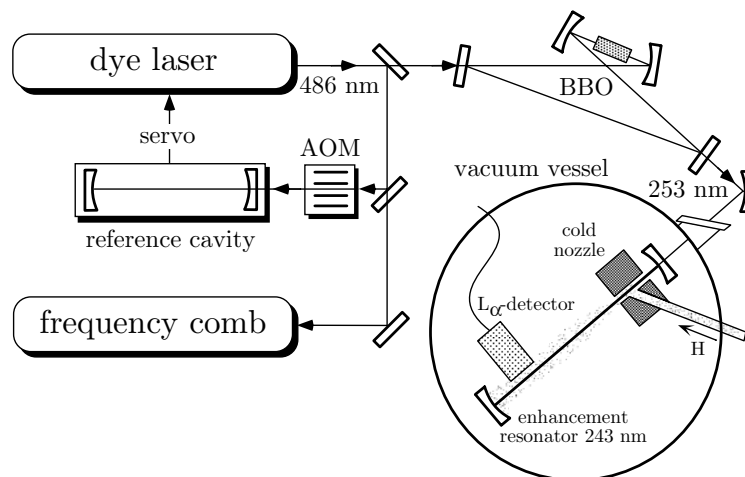


Fig. 7. – Exciting the hydrogen $1S$ - $2S$ transition with two counterpropagating photons in a standing-wave field at 243 nm. This radiation is obtained from a dye laser frequency doubled in a BBO crystal and stabilized to a reference cavity. While scanning the hydrogen resonance the frequency of this laser is measured with a frequency comb to be $2\,466\,061\,413\,187\,074$ (34) Hz for the hyperfine centroid [74].

4.1. Hydrogen and drifting constants. – The possibility to readily count optical frequencies has opened up new experimental possibilities. High-precision measurements on hydrogen have allowed for improved tests of the predictions of quantum electrodynamics and the determination of the Rydberg constant [14]. As the simplest of all stable atomic systems, the hydrogen atom, provides the unique possibility to confront theoretical predictions with experimental results. To explore the full capacity of such a fundamental test, one should aim for the highest possible accuracy so that measuring a frequency is imperative as explained in the introduction. At the same time one should use a narrow transition line that can be well controlled in terms of systematic frequency shifts. The narrowest line starting from the $1S$ ground state in hydrogen is the $1S$ - $2S$ two-photon transition with a natural line width of 1.3 Hz and a line Q of 2×10^{15} .

At the Max-Planck-Institute für Quantenoptik (MPQ) in Garching measurements of this transition's frequency around 2466 THz has been improved over many years [13, 19, 74]. The hydrogen spectrometer used for that purpose is sketched in fig. 7. It consists of a highly stable frequency-doubled dye laser whose 243 nm radiation is enhanced in a linear cavity located in a vacuum vessel. The emission linewidth of the dye laser is narrowed to about 60 Hz by stabilizing it to an external reference cavity. This stabilization also reduces the drift rate below 1 Hz per second. The linear enhancement cavity ensures that the exciting light field is made of two counterpropagating laser fields, so that the Doppler effect is cancelled to first order. Hydrogen atoms are produced in a gas discharge and ejected from a copper nozzle kept at a temperature of 6 K. After propagating the length of 13 cm, the excited atoms are detected by quenching them to the ground state in an electric field. The Lyman- α photon at 121 nm released in this process is then detected with a photomultiplier.

The optical transition frequency was determined in 1999 [13] and in 2003 [74] with a

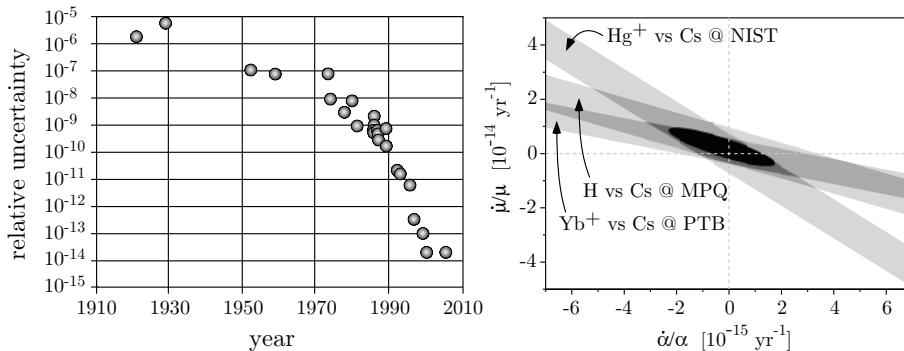


Fig. 8. – Left: a century of hydrogen data. Since the early 1950’s when quantum electrodynamics was developed, measurements have been improved by almost 7 orders of magnitude and still no serious discrepancy has been discovered. Right: from the observation of transitions in single trapped ytterbium and mercury ions and the $1S$ - $2S$ transition over several years, upper limits on small possible variations of the electromagnetic and the strong interaction can be found. The latter appears here as a variation of the cesium nuclear magnetic moment μ measured in units of Bohrs magneton.

frequency comb that was referenced to a transportable cesium fountain clock from LNE-SYRTE, Paris [75]. At this time the repeated measurement did not yield an improved value for the $1S$ - $2S$ transition frequency. Lacking a suitable laser cooling method is a particular problem for the light hydrogen atom. Even after thermalizing with the cold nozzle to 6 K, the average atomic velocity is $v = 360$ m/s causing a second-order Doppler effect of $0.5(v/c)^2 = 7 \times 10^{-13}$ that needs to be accounted for. In addition the brief interaction of the atoms with the laser cause a variety of problems and can distort and shift the lineshape in an unpredictable way on the 10^{-14} level. In addition, because of the limited interaction time, larger laser power has to be used for a sufficient excitation rate. This increases to ac Stark shift and cause problems when extrapolating to zero laser power to find the unperturbed transition frequency. Nevertheless the inaccuracy is only about an order of magnitude larger than the best atomic clocks. A historic summary of hydrogen spectroscopy is given at the left side of fig. 8. As a remarkable aspect it should be noted that before the introduction of quantum electrodynamics basically every order of magnitude that measurement improved, required a new theory or at least some refinement. Quantum electrodynamics by now has resisted a gain of almost 7 orders of magnitude without such a refinement. This is probably unprecedented for any physical theory. The development is summarized at the left panel of fig. 8.

The two comparisons of the hydrogen $1S$ - $2S$ frequency with the LNE-SYRTE fountain clock may also be used to derive upper limits of possible slow variations of the fundamental interactions. The question of a possible time variation of fundamental constants⁽⁸⁾ was first raised in 1937 by P. A. M. Dirac, where he speculated that fundamental constants could change their values during the lifetime of the universe [77]. The traditional way to search for such a phenomenon is to determine the value of say the fine-structure constant as it was effective billions of years ago. For this purpose atomic absorption lines

⁽⁸⁾ For a review on this subject see ref. [76].

of interstellar clouds back-illuminated by distant quasars have been analyzed [78-81]. In a related method, the only known natural nuclear fission reactor that became critical some 2 billion years ago at Oklo, Gabon has been investigated [82-84]. Analyzing the fission products the responsible cross-sections and from that the fine-structure constant at the time this reactor was active can be deduced.

Now using frequency combs, high-precision optical standards can be compared with the best cesium clocks on a regular basis. Besides the hydrogen transition, the best monitoring data of this type so far derives from comparisons of narrow lines in single trapped mercury [17] and ytterbium [18] ions with the best cesium atomic clocks. Remarkably, the precision of these laboratory measurement makes it possible to reach the same sensitivity within a few years of monitoring that astronomical and geological observations require billions of years of look back time. The laboratory comparisons address some additional issues: Geological and astronomical observations may be affected by systematic effects that lead to partially contradicting results (see refs. [78,81,85,86] for contradicting results on quasar absorption and [83,84] for Oklo phenomenon data).

In the laboratory systematics can be investigated or challenged, and if in doubt, experiments may be repeated given the relative short time intervals. So far atomic transition frequencies have been compared with the cesium ground-state hyperfine splitting, which is proportional to its nuclear magnetic moment. The latter is determined by the strong interaction, but unlike the electronic structure, this interaction cannot easily be expressed in terms of the coupling constant. Lacking an accepted model describing the drift of the fundamental constants, it is a good advice trying to analyze the drift data with as few assumptions as possible. In previous analysis of the Oklo phenomenon, for example, it was assumed that all coupling constants but the fine-structure constant are real constant in time. However, if grand unification is a valid theory, at least at some energy scale, all coupling constants should merge and drift in a coordinated way [87]. Therefore the possibility that the cesium ground-state hyperfine splitting, *i.e.* the pace of the fountain clocks may have changed, should not be ruled out by the analysis. In this sense any of the optical frequencies monitored relative to the cesium clock can only put limits on the relative drift of the electromagnetic and the strong coupling constant. Fortunately the three mentioned comparisons show different functional dependences on the fine-structure constant leading to different slopes in a two-dimensional plot that displays the relative drift rates of the coupling constants (see right panel of fig. 8). The region compatible with this data is consistent with no drift at all, at a sensitivity level only a factor 2 away from the best astronomical observations that have been detecting a statistically significant variation [19]. It should be noted though that without a model for the drift, linearity in time cannot be assumed, so that the laboratory measurements do not even compare with the astronomical observations as they probe on different epochs. In the near future direct comparisons between different optical transitions will provide much better data because the cesium clock drops out and some optical transitions are getting more accurate than even the best cesium fountain clocks [9, 88]. The frequency comb also allows this type of frequency comparison by locking one of the optical modes ω_n to the first optical reference and measuring the second with another mode $\omega_{n'}$. Ideally the carrier envelope offset frequency is stabilized to an integer fraction $1/m$ of the repetition rate, so that the ratio of the two optical frequencies derives as [89].

$$(27) \quad \frac{\omega_{n'}}{\omega_n} = \frac{n + 1/m}{n' + 1/m}.$$

No radio frequency enters in this comparison and possible beat notes can also be referenced to the repetition rate. Probably the most advanced experiment of this type would be the comparison of narrow transitions in aluminum and mercury ions operated in the group of J. Bergquist at NIST, Boulder. These standards are now reaching a reproducibility within a few parts in 10^{17} [9]. To put this in perspective, it should be noted that the gravitational red shift at the Earth's surface is $g/c^2 = 1.1 \times 10^{-16} \text{ m}^{-1}$.

4.2. Fine structure constant. – Besides helping to detect a possible variation of the fine-structure constant α , the frequency combs are also useful to determine its actual value. All experiments to determine α have in common that a quantity that depends on it, is measured. The fine-structure constant is then determined by inverting the theoretical expression which usually comes as a power series in α .

As mentioned above, precision spectroscopy of hydrogen has led to an accurate experimental value for the Rydberg constant. Using all the available hydrogen data, *i.e.* the $1S$ - $2S$ transition frequency and other less precise measurements [14], a value with an uncertainty of only 7 parts in 10^{12} is obtained [14, 90]. The Rydberg constant R_∞ can be traced back to other constants according to

$$(28) \quad R_\infty = \frac{\alpha^2 m_e c}{2h},$$

so that the fine-structure constant α is derived as precise as m_e/h , the electron mass divided by Planck's constant, is known. This is because the speed of light c has a defined value within the SI units and enters with no uncertainty.

Currently the most precise measurement of the fine-structure constant has an uncertainty of 7 parts in 10^{10} [91]. This measurement is based on an experimental value of the electrons gyromagnetic ratio or more precisely its deviation from 2. This quantity can be calculated with quantum electrodynamics with comparable accuracy in terms of a power series in α . By comparison with the measured value, the fine-structure constant is determined.

Because α scales the strength of all electromagnetic interactions, it can in principle be determined with a large number of different experiments. Currently the second best method is based on the recoil an atom, such as cesium [92] or rubidium [93], experiences when absorbing an optical photon. Momentum conservation requires that the transition frequency is shifted by the kinetic energy associated with the photon momentum $\hbar k$ and the atomic mass M :

$$(29) \quad \Delta\omega = \frac{\Delta E}{\hbar} = \frac{\hbar k^2}{2M} = \frac{\hbar}{M} \frac{\omega^2}{2c^2}.$$

Measuring this recoil shift $\Delta\omega$ and the optical transition frequency ω yields a value for M/h . The recoil shift is typically only a few kHz on top of the transition frequency of several 100 THz. Therefore high-resolution optical frequency measurements are mandatory. To obtain α from (28) one additionally needs to know the mass ratio m_e/M . Atomic mass ratios can be measured very precisely by comparing their cyclotron frequencies in Penning traps [94]. In fact such an effort was the motivation for the first frequency comb measurement performed with a femtosecond laser [15]. Note that all ingredients for deriving α via eq. (29) are obtained from precision frequency measurements, two of which optical frequencies.

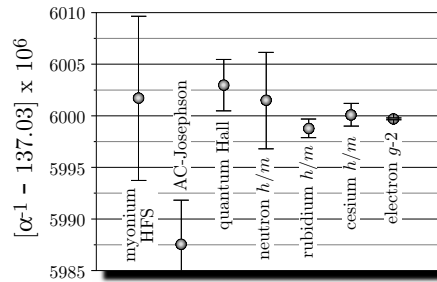


Fig. 9. – The agreement of various values, derived from different experiments is a crucial test for quantum electrodynamics. Currently the values nicely agree within their assigned uncertainty, except the one derived from the Josephson effect. For further details see [91, 90].

Even though less precise than the gyromagnetic ratio, the recoil measurements are important when it comes to testing of quantum electrodynamics. In general any theory that uses N parameters can only be said to have a predictive character if at least $N + 1$ different experimental outcomes can be verified. The first N measurements are only fixing the parameters. In this context here the available data may be interpreted in a way where the gyromagnetic ratio fixes α without any verification of the theory. The recoil measurements are then interpreted as a test quantum electrodynamics, or the other way around. Currently the gyromagnetic ratio fits very well with recoil measurements in cesium and rubidium and other measurements. As fig. 9 shows, the only exemption may be a value derived from the Josephson effect, which does not seem to fit within its assigned error bar.

Finally it should be mentioned that of course quantum electrodynamics could be correct while calculations and/or measurements have some undetected errors. Calculating the electron gyromagnetic ratio as a function of α has so far used 891 Feynman diagrams. One might think that the recoil measurements does not show this problem, but deriving the Rydberg constant from hydrogen data involves a similar complex evaluation [95].

4.3. Optical frequencies in astronomy. – In connection with cosmological search for a variation of what we believe are fundamental constants, optical frequency measurements are required on samples in the sky and on Earth as reference. Yet another type of observation relies on precise optical frequency measurements. To detect extrasolar planets the most powerful method has been to measure the changing recoil velocity of its star during the orbital period. These recoils velocities are rather small unless a massive planet in close orbit is considered. This is the reason why mostly “hot Jupiters” are among the roughly 200 extrasolar planets detected so far. The lightest of those planets possesses about 10 Earth masses. The wobble that our planet imposes on the motion of our Sun has a velocity amplitude of only $v_E = 9$ cm/s with a period of one year of course. Because Earth and Sun maintain their distance as they go around their common center of mass, this motion is invisible from Earth. On the other hand, it can be detected at other stars, where it is superimposed with the center-of-mass motion of that system of typically 100’s of km/s and the motion of the Earth around the Sun. To detect Earth-like planets that orbit sun-like suns with the recoil velocity method, a relative Doppler shift of $v_E/c = 3 \times 10^{-10}$ needs to be measurable. Converted to visible radiation of say 500 THz this requires a

resolution of 150 kHz and the same reproducibility after half the orbital time.

Spectral lines from atoms and ions from interstellar clouds and the surface of stars are subject to strong line broadening due to collisions and the Doppler broadening of typically several GHz due to their thermal motion. They are measured with telescopes like the Very Large Telescope operated by the European Southern Observatory which can be connected to an Echelle-type spectrometer for high resolution. Given these rather broad lines, the required spectral or velocity resolution can be obtained only by using the statistics of many lines observed simultaneously. It requires a spectrometer with very small irregularities in the calibration curve. So far the rather irregular line spectrum Tr-Ar lamps have been used for that purpose, with large spectral gaps. Using a frequency comb for this purpose appears to be the optimum tool, both in terms of providing an equidistant dense calibration and for allowing long-term reproducibility that goes well beyond the typical life time of an individual spectrometer [96]. The latter property derives from the possibility to reference to a precise clock. In this case even a simple GPS disciplined rubidium clock suffices for the required 3×10^{-10} reproducibility to detect Earth-like extrasolar planets.

In the long run one may even think about direct heterodyne detection with a frequency comb. In this scheme the star light is mixed with the frequency comb on a fast photo detector producing a radio frequency spectrum identical to the optical spectrum but shifted by the optical frequency. Signal processing can then be done with a radio frequency spectrum analyzer rather than with an optical spectrometer. This type of detection is known for producing shot noise limited signals and is used to demonstrate noise levels below the shot noise limit with squeezed light. The frequency comb can provide a large number of optical local oscillators to shift any optical component within its span to the radio frequency domain.

4.4. Reconstructing pulse transients and generating attosecond pulses. – The application of the frequency combs has also enabled advances in another field as it allows the possibility for stabilizing the carrier envelope phase [3, 6]. According to fig. 2 and eq. (8), a pulse train with a vanishing carrier envelope frequency ω_{CE} has a fixed phase of the carrier with respect to the envelope. This means that all the pulses have the same electric field. With the technique of self-referencing this can be readily accomplished. However, even though the electric-field transients of the pulses are identical in this case, it is unknown what value the carrier envelope phase actually assumes upon stopping its pulse-to-pulse slippage. In order to figure out at what position the carrier envelope phase has actually stopped, all delays in the system including the optical path delays have to be known. Taking into account that the latter progresses by 2π for each wavelength propagation distance such an attempt seems unrealistic.

To detect the value of the carrier envelope phase very short pulses that drive processes which depend on the electric field in high order are used. The left-hand side of fig. 10 shows two extreme values of the carrier envelope phase that correspond to a “cos” and a “sine” pulse. Close observation of the field transients reveals that the peak electric field slightly depends on the carrier envelope phase. In addition the duration of the optical carrier cycle changes slightly due to the steep pulse envelope when measured say between two field maxima. These effects are largely enhanced if the pulses are short and can be detected using highly non-linear processes such as “high harmonic generation” [100-102] or “above threshold ionization” [103]. High harmonics are generated if pulses of high intensity are focused into a noble-gas jet and are emitted in a nicely collimated laser-like beam. Very short wavelengths up to the soft-X-ray regime have been produced this

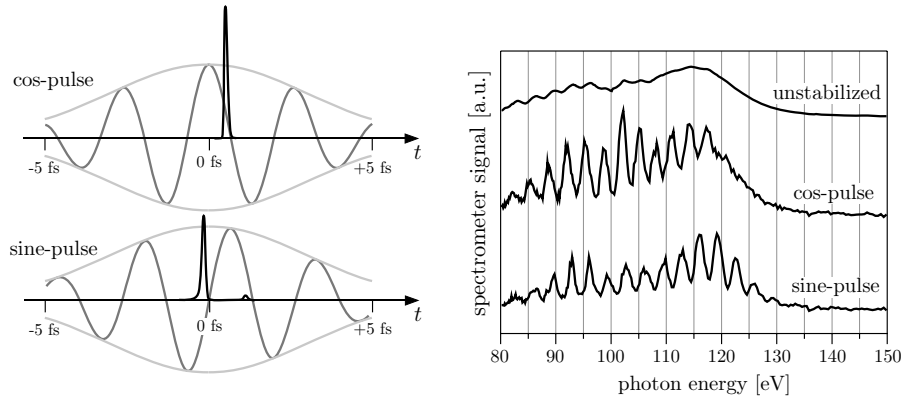


Fig. 10. – Left: infrared driving pulses of high intensity and the calculated intensity of high harmonic radiation around the short wavelength cut-off spectral region for two different values of the carrier envelope phase [97]. Whereas a “sine” pulse creates two high harmonic pulses, a “cos” produces a single isolated attosecond pulse [98]. Right: measured spectra (different intensity) for the two values of the carrier envelope phase. It is seen that the cut-off region loses its periodicity with the carrier wave as expected for single isolated attosecond pulses. Figures adapted from ref. [97,99].

way [104]. Added to the left-hand side of fig. 10 is the calculated high harmonic radiation at a narrow bandwidth around the high-frequency cut-off. Two important aspects are realized from this: For “cos” driving pulse the high harmonic pulse is much shorter than one cycle of the generating field. So by stabilizing the carrier envelope phase to the proper value (“cos” drive pulses) single isolated attosecond could be produced for the first time [97,99]. Secondly the high-harmonic spectrum reveals whether the carrier envelope phase has been fixed at the proper value or not. A “sine” drive pulse creates two high-harmonic pulses, that have almost but not quite the time separation given by the carrier frequency. For this reason the spectrum shows well-separated peaks even in the cut-off spectral region. However the positions of these peaks are not exactly harmonics of the infrared driving field. In contrast to that, a “cos” produces a shifted harmonic spectrum that loses its periodicity in the cut-off region. This is because it belongs to a single isolated attosecond pulse [98], as show in the upper left part of fig. 10. It should be noted that all of this applies only when the high-harmonic radiation is properly filtered. This should be obvious for two reasons: Only the highest harmonics possess enough non-linearity to distinguish the carrier envelope phase settings. Secondly when attosecond pulses are generated, their carrier frequency must be significantly larger than the inverse pulse duration.

Not only that the detection and stabilization of the carrier envelope phase allowed the production of attosecond pulses for the first time, it also allowed to completely recover the electric-field transients of ultrashort pulses. The work in that direction relied on measuring the pulses autocorrelation which, together with the determination of the carrier envelope phase via spectral analysis of high harmonic allows the calculation of the field transient [99]. A more direct measurement uses cross correlation between attosecond pulses generated the way described above with the driving pulses. In this way the field transient of the latter can be sampled with a temporal resolution significantly shorter

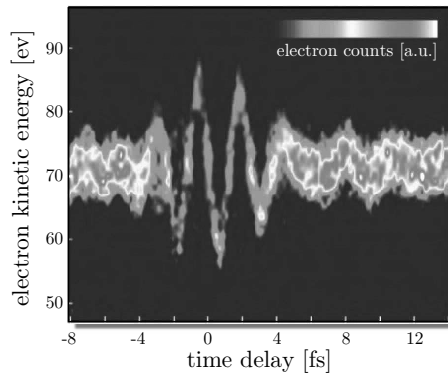


Fig. 11. – Cross-correlating attosecond pulses with the driving fundamental infrared laser pulses. The attosecond pulses are used to ionize atoms and the liberated electrons are accelerated by the instantaneous field of the infrared pulses. By changing the delay between the pulses, the electric-field transient can be sampled with sufficient temporal resolution. Figure courtesy of E. Goulielmakis *et al.* [105].

than one optical cycle [105]. Figure 11 shows the result of such a measurement.

4.5. Frequency comb spectroscopy. – While for high-resolution spectroscopy of transitions such as the hydrogen $1S-2S$ single-mode lasers are currently employed, many transitions of fundamental interest occur at wavelengths too short for state-of-the-art continuous wave lasers. The boundary is set by the transparency range of the existing non-linear crystals. The crystal material that is useful for the shortest wavelength is BBO (β -barium-borate), with a transparency cut-off at about 190 nm. Only with pulsed lasers it is possible to efficiently convert into new regimes in the vacuum UV (200–10 nm), extreme UV (30–1 nm) and possible even the soft X-ray (< 10 nm)⁽⁹⁾. The process that allows this is high-harmonic generation [100–102], that was already discussed in the last section. For a long-time-pulsed lasers and high-resolution spectroscopy seemed to exclude each other because of the large bandwidth associated with short pulses. However, coherent train of pulses as compared to isolated or non-coherent pulses (say from a Q-switched laser) have quite distinct spectra. The coherent pulse train generated from a mode locked laser consists of narrow modes. It was shown in subsect. 2.3 that the Fourier and the Schawlow-Townes limit of the linewidth of an isolated mode is identical to the linewidth of a single-mode laser of the same type with the same average power. This opens the possibility to combine the high peak powers of mode-locked lasers, suitable for frequency conversion, with the properties of a sharp laser line produced by a single-mode laser.

One obvious problem with this approach is the limited power per mode in a broad frequency comb. Given an octave-spanning comb, as required for simple self-referencing, this can easily drop below 100 nW in practice. In addition the unused modes may cause excess ac Stark shift that poses a problem in high-accuracy measurements. Still these problems can be handled as demonstrated in ref. [106]. Another solution, at least for the

⁽⁹⁾ These spectral ranges are not used in a unified way and partially overlap.

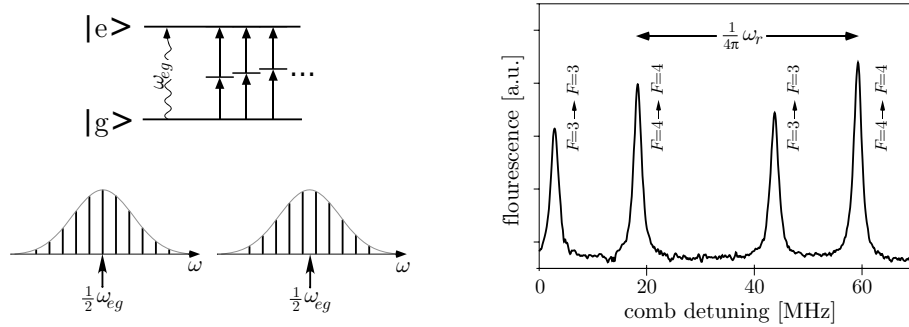


Fig. 12. – Left: the modes of a frequency comb add up to largely enhance the transition amplitude between levels $|g\rangle$ and $|e\rangle$ if only one of the central modes is resonant with a two-photon transition or that resonance occurs exactly half ways between two modes. Right: as an example, frequency comb excitation of the $6S$ - $8S$ two-photon resonance is shown as the frequency comb is tuned across it. The hyperfine doublet with angular momentum F repeats with half the repetition rate of $\omega_r/2 = 2\pi \times 41$ MHz as expected from the resonance conditions [107].

UV spectral region, is to combine a fs mode-locked laser as a precise frequency reference with a ps mode-locked laser for spectroscopy [107]. The latter type of lasers can be converted in wavelength with efficiencies approaching unity even in single pass.

Yet an even better idea is to employ a two-photon transition as initially proposed by Ye. F. Baklanov and V. P. Chebotayev [108]. At first glance it seems that a two-photon transition does require even more power. However it is straightforward to see that in this case the modes can sum up pairwise such that the full power of the frequency comb contributes to the transition rate: suppose the frequency comb is tuned such that one particular mode $n\omega_r + \omega_{CE}$, say near the center, is resonant with the two-photon transition. This means that two photons from this mode provide the necessary transition energy of $\omega_{eg} = 2(n\omega_r + \omega_{CE})$. In this case the combination of modes with mode numbers $\{(n-1, n+1), (n-2, n+2), (n-3, n+3), \dots\}$ are also resonant as they sum up to the same transition frequency. In fact all modes contribute to the transition rate in this way. The same applies if the two-photon resonance occurs exactly half ways between two modes. Figure 12 gives more details and a sample curve obtained from the $6S$ - $8S$ two-photon resonance in cesium at 822 nm. It can be shown for unchirped pulses that the total two-photon transition rate is the same as if one would use a continuous laser with the same average power [108]. If the pulses are chirped, transition amplitudes corresponding to the various combinations of modes do no longer add up in phase so that the total transition rate is lower [109].

Experimentally frequency comb spectroscopy has been pioneered by J. Eckstein [110] and M. J. Snadden [111] and coworkers on sodium and rubidium, respectively, directly with a mode-locked laser. While the former experiment was still a factor 2.5 short of the 1.6 MHz natural linewidth, the latter reached the natural linewidth of 300 kHz. The main difference between the two measurements is that Snadden and coworkers used laser-cooled atoms in a magneto-optical trap.

This comparison reveals one disadvantage of the method. There may be a significant time-of-flight broadening because the Doppler free signal only emerges from atoms within the pulse collision volume for counterpropagating pulse trains. Atoms that fly through

this volume can only absorb a limited number of pulses that cause the line broadening effects described in subsect. 2'3. To obtain a narrow resonance, it is therefore important to apply many pulses, ideally for a time that exceeds the inverse natural linewidth. When using fs pulses the collision volume may be smaller than 1 mm so that the atoms must be laser cooled and/or trapped as in ref. [111] to reach the natural linewidth. Note that the time-of-flight broadening may also be understood as a residual first-order Doppler effect. This comes about because, unlike the single-mode case, the Doppler shift $k_1 v$ and $-k_2 v$ for counterpropagating beams with wave numbers k_1 and $-k_2$ does not exactly compensate for the motion of the atom with velocity v . However for any residual first-order Doppler shift there exists a component obtained by exchanging the wave numbers $k_1 \rightleftharpoons k_2$ that possess the opposite shift. Hence a pure broadening and no shift results just as in the time domain description. This is certainly an advantage.

In the meantime several other groups have used laser-cooled atoms for frequency comb spectroscopy [112, 113]. S. Witte and coworkers used UV pulses at 212 nm generated in conventional non-linear crystals to excite a two-photon transition in krypton [114]. In this work only 3 pulses could be applied to the atoms so that the expected linewidth was about one third of the repetition rate or 23 MHz. Indeed that is about the observed linewidth which compares to the natural linewidth of 6.9 MHz. This experiment demonstrates the principle, knowing that improvements by many orders of magnitude should be possible. However, realizing these disadvantages of frequency comb spectroscopy, it appears advisable to use a continuous wave laser whenever possible. On the other hand, if there is no laser of this kind, frequency comb spectroscopy can become a very powerful method. One of the first demonstration in the short, so far inaccessible wavelength range, uses the ninth harmonic of a titanium-sapphire laser generated in a xenon gas jet to perform Ramsey-type spectroscopy on krypton at 88 nm [115]. The Ramsey method is identical to frequency comb spectroscopy with two pulses and produces narrow lines only when the two pulses come at a long delay (low repetition rate). In the meantime the same Ramsey-type spectroscopy has also been demonstrated at a one-photon transition in xenon at 125 nm [116]. The required radiation was obtained as the third harmonic produced in a gas cell. In this experiment the "repetition rate", *i.e.* the time separation between the Ramsey pulses was varied to increase the resolution.

Using high harmonics from titanium-sapphire lasers several 100 octaves of laser radiation may be addressed without gaps. Given the large tunability of these lasers allows to shift between the harmonics seamlessly. Therefore it might become possible to use a single laser system to cover everything from the near infrared to soft X-rays with atomic clock resolution. A possibility that seems out of reach for single-mode lasers. For such a general laser system there is yet another obstacle that needs to be solved. So far long pulse trains of many pulses at very short wavelengths with a high repetition rate necessary to resolve the modes have been contradicting requirements. This is because all methods up to very recently, that allowed to reach the necessary intensity for high-harmonic generation of typically 5×10^{13} W/cm², effectively concentrate the available average power in fewer pulses per second. For this the repetition rate is typically reduced to the kHz regime. The modes of the resulting dense frequency comb would be very difficult to resolve. Even if the time-of-flight broadening could be reduced, say by using trapped ions and transitions with narrow natural linewidths, the requirements on the laser system would be difficult to achieve. For this reason a method allowing the production of high-harmonic radiation with MHz repetition rates was sought. The solution to this problem was to use an enhancement resonator for the driving pulses with an intracavity gas jet for high-harmonic generation [117, 118]. This method is similar

to resonantly enhanced second-harmonic generation that has been used for many years. However, there are several extra requirements that need to be fulfilled in order to resonantly enhance fs pulses. First of all the pulse round trip time in that cavity has to be matched to repetition rate of the laser. In fact this is not difficult to accomplish and standard continuous wave locking schemes can be applied to stabilize the frequency comb to the modes of the enhancement resonator. Somewhat more difficult is it to prevent the pulse stored in the enhancement resonator from reshaping, or more precisely to reshape it such that after one round trip it will match the next pulse from the laser. As discussed in subsect. 2.1 this means that the carrier envelope phase shift of the cavity has to be the same as for the laser and higher-order dispersion has to be suppressed. In the frequency domain this simply means that the modes of the enhancement resonator must be equidistant in frequency just as the frequency comb is. In this case all modes can resonate at the same time. So far this problem has not been solved completely, so that the high-harmonic intensity generated this way still seems too low for a reasonable transition rate in stored ions. Fortunately this process scales very favorably with the driving intensity I . The so-called plateau harmonics scale with number of fundamental photons required for ionization, which is $\propto I^9$ for Xe driven with a titanium-sapphire laser around 800 nm.

5. – All optical clocks

Most likely the first time piece of mankind was the periodic movement of a shadow cast by a fixed object. The daily period would measure the Earth rotation and the superimposed annual period could be used to find the solstice and measure the length of the year in units of days. Later other periodic phenomena have been used. For an operational clock the periodic phenomena or oscillator has to be completed by a counter that keeps track of the number of periods. The early sundials had a human operator for counting the days. Later pendulum clocks used mechanical counters and today's precise clocks such as quartz or atomic clocks have electronic counters. If we look at the history of time keeping, it becomes obvious that clocks got more accurate as the oscillation frequency increased. One simple reason for that is that higher oscillation frequencies can slice time into finer intervals. Similar to a ruler that improves with the density of length marks.

The two most important properties of clocks are accuracy and stability. The former describes at what level two identically constructed clocks agree. The clocks stability, on the other hand, measures how well a particular clock maintains its pace. Both, accuracy and stability are determined by comparing at least two clocks and are limited by many factors such as the oscillators sensitivity to external perturbations. An increased oscillator frequency helps to improve stability. As an example consider the Earth rotation represented by a sundial and a good quartz oscillator. Whereas the two oscillators may be comparable in terms of accuracy, it would be much more difficult to measure a period of one second with a sundial than with a quartz oscillator that typically vibrates 32 768 times a second. Even faster than the vibration of a quartz standard is the precession of the Cs nuclear magnetic moment in the magnetic field of its electrons. This frequency has been defined within the International Systems of Units (SI) to be exactly 9 192 631 770 Hz.

To quantify the mutual stability of two oscillators a statistical analysis of a set of subsequent phase comparisons, obtained by averaging over time intervals τ , is used. For this purpose one may not use the standard deviation because it does not converge if the

two clocks have slightly different frequencies, which is almost always the case. Instead the statistical analysis is done in terms of the Allan variance $\sigma(\tau)$ [119]. Having eliminated all other sources of instability an atomic oscillator, that obeys the laws of quantum mechanics, possesses the following expression for the Allan variance:

$$(30) \quad \sigma(\tau) = \frac{\Delta\omega_0}{\pi\omega_0} \sqrt{\frac{T_c}{2N\tau}}.$$

Here the frequency and the linewidth of the transition are given by ω_0 and $\Delta\omega_0$, respectively and the number of oscillators (atoms or ions) and the interrogation time is given by N and T_c . Modern Cs atomic clock can be operated close to that limit [75]. Of course the Allan variance will not reduce indefinitely for longer averaging times as suggested by the quantum limit. At some point varying systematic effects will set in and prevent further reduction. Current state-of-the-art Cs clocks need to be averaged for hours to reach that limit at around one part in 10^{15} . If one sets out to reach an accuracy of one part in 10^{18} , which is the predicted systematic uncertainty for some optical transitions, the necessary averaging times would extend by 6 orders of magnitude according to eq. (30). This of course is no longer useful for any practical purpose.

Fortunately the same equation suggests that one can make up for this by increasing the transition frequency ω_0 as illustrated above. At first glance it may seem that reducing the linewidth $\Delta\omega_0$ by choosing a narrow transition would serve the same purpose. In principle one could pick an almost arbitrary narrow transition, such as between ground-state hyperfine levels that basically live forever or highly forbidden transition such as the $\text{Yb}^+ \ ^2\text{S}_{1/2} \rightarrow \ ^2\text{F}_{7/2}$ transition, whose upper level lives for about ten years [120]. However this means that there will be one photon of information per lifetime available at most, assuming 100% detection efficiency. For this reason a much better strategy is to use a larger transition frequency such as an optical transition leaving the linewidth, *i.e.* the inverse transition rate fixed. Ideally one would choose an optical transition that represents an oscillator at frequency of several hundreds of terahertz. Operating at these high frequencies would have been possible after tremendous advances in laser spectroscopy in the 1970s that ultimately resulted in trapped atom and ion standards [121] in the 1980s. What was missing though was an efficient counter that keeps track of these fast oscillations. When it became possible to count these oscillations with the so-called harmonic frequency chains in the early 1970s [122], physicists started to seriously thinking of running an optical clock. However, working with these counters was so tedious that most of the harmonic frequency chains never reached the stage where they could operate continuously even for minutes. So it was decided to use them only to calibrate some chosen frequencies, like iodine or methane stabilized HeNe lasers, that could then be reproduced in other labs that could not provide the tremendous resources required for setting up a harmonic frequency chain. The calibrated lasers were then mostly used as wavelength references in interferometers for the realization of the meter and in some scientific experiments as frequency references.

With the introduction of femtosecond frequency combs a reliable running optical clock became reality. In particular the fiber-based frequency combs can now run for months without touching them [63]. In addition excess noise observed in these lasers has recently been suppressed to the level of titanium-sapphire laser [64]. One of the first set-ups that deserved the term ‘‘optical clock’’ used a transition at 1064 THz in a trapped single mercury ion operated at NIST [89]. For a device deserving this name one would ask for some requirements on its accuracy and its ability to be operated long enough to

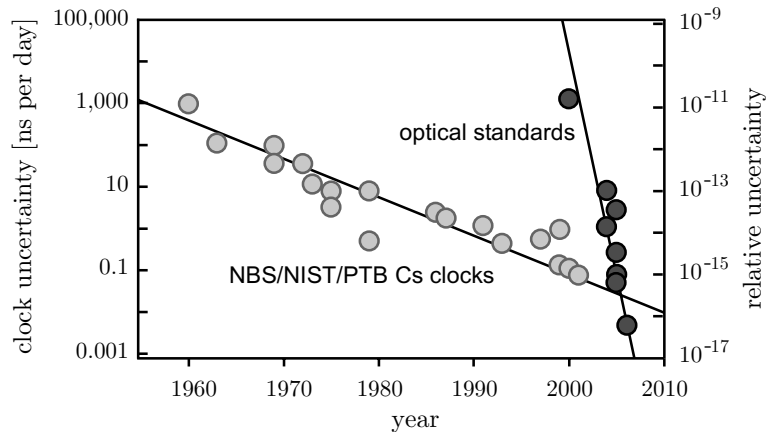


Fig. 13. – The historic comparison of radio frequency standards reveals that just about now the optical standards seem to take over the lead. The current lowest uncertainty is reached with the Hg^+ clock at NIST [9] with an estimated standard uncertainty of 7 parts in 10^{17} .

calibrate a hydrogen maser for example. The NIST Hg^+ clock can be operated repeatedly with an uncertainty low enough such that comparison with an ensemble of very stable hydrogen masers resulted in an Allan variance of the latter [9]. By now many national standard institutes are working on optical atomic clocks. The Physikalisch-Technische Bundesanstalt, Germany (PTB) on Yb^+ [123], the National Physics Laboratory, UK (NPL) on Sr^+ and Yb^+ [11] and the Laboratoire national de métrologie et d’essais—Système de Références Temps-Espace, France (LNE-SYRTE) on neutral Sr [124] to name a few. The tremendous progress of the optical standards made since frequency combs were introduced is summarized in fig. 13.

To operate a frequency comb as a clockwork mechanism one might stabilize its nearest mode ω_k to the clock transition. Similar to the frequency ratio scheme of eq. (27), the carrier envelope offset frequency and possibly any local oscillator used in the stabilization, can be locked to an integer fraction m of the repetition rate [89].

$$(31) \quad \omega_k = k\omega_r + \omega_{\text{CE}} = \omega_r(k + 1/m).$$

The countable clock output is then obtained in form of the pulse repetition rate that is given by the optical reference ω_k divided by $k + 1/m$. No other reference frequency besides the optical reference is required at this point as it should be for a real clock. In particular there is no radio frequency source required other than the repetition rate. To use the repetition rate in this way as a radio frequency generator is advantageous as it can be shown that, on a short time scale, this frequency is more stable than a good synthesizer even for a free-running laser [39].

6. – Optical frequency standards

Since the redefinition of the unit of length, the meter, in the International Systems of Units (SI) in 1983 by the 17th General Conference on Weights and Measures (CGPM) [125] the speed of light is fixed by definition to $c = 299\,792\,458$ m/s. With the

general relation $c = \lambda \times \nu$ any radiation emitting device whose frequency ν and hence its wavelength λ is stable and can be traced back to the frequency of the Cs clock can be used as a frequency standard or a wavelength standard. Such frequency standards have been used for decades for interferometric length metrology. The International Committee of Weights and Measures (CIPM) has therefore recommended a list of evaluated frequency standards, *i.e.* the so-called *Mise en Pratique* for the definition of the Metre [126] which has been updated on several occasions [125, 127, 128].

The first frequency standards in this list were mainly gas lasers whose frequencies were stabilized to the saturated absorption of suitable transitions in molecules. The selected molecules by natural coincidence have transitions whose frequencies are located in the tuning range of the laser. The most prominent examples are the CH₄ stabilized He-Ne laser at 3.39 μm , the OsO₄ stabilized CO₂ laser at 10.3 μm and the I₂ stabilized Ne-He or Nd:YAG lasers at 632 nm and 532 nm, respectively. While the first two of these lasers probably have the best reproducibility of all lasers stabilized this way, the much more compact and transportable iodine stabilized laser has been the working horse in length metrology for quite some time. The best of these lasers are reproducible within a few parts in 10¹³ and therefore cannot compete with the current Cs atomic clocks.

The possibility to cool atoms and ions by laser radiation has led to optical frequency standards that could rival the best microwave clocks. In these laser-cooled quantum absorbers suitable narrow transitions can be interrogated that are no longer excessively broadened and shifted by effects associated with the velocity of the absorbers, *e.g.*, the short interaction time and the influence of the second-order Doppler effect.

Optical frequency standards employing ions or neutral atoms as the frequency references show distinctive differences. Ions can be stored in a so-called radio frequency trap where an alternating electric voltage is applied to a suitable arrangement of electrodes that results in a net force onto the ions directed towards the field-free center of the ion trap. Since alike charged ions repel each other only a single ion can be kept in the center whereas the non-vanishing field outside the center in general shifts the transition frequency. Most accurate ion frequency standards therefore store only a single ion which, however, leads to a very weak signal.

To produce a much stronger signal and an associated much higher stability as compared to single ions ($N = 1$ in eq. (30)) the second type of laser-cooled optical frequency standards uses clouds of millions of neutral atoms. In this case though collisions between the atoms may result in uncontrollable shifts in frequency. In other words, so far (but not necessarily in the long run) single-ion standards have high statistical but low systematic uncertainties whereas neutral-atom standards have excellent short-term stability but poorer systematic properties.

The recent progress with optical frequency standards in the mean time motivated the CIPM to recommend in autumn 2006 four optical frequency standards (see table I) that can be used as “secondary representations of the second” and be included into the new list of “Recommended frequency standard values for applications including the practical realisation of the metre and secondary representations of the second”. The phrase “secondary representations” takes into account that the frequency of such an optical frequency standard can never surpass the accuracy of the primary standard of time and frequency, the Cs clock, but that it might be very important also for time keeping to use optical clocks because of their better stability. We will discuss the frequency standards of table I in more detail in the following subsections.

The uncertainties given in table I are in general larger than the uncertainties presented

TABLE I. – *Optical clock transitions recommended by the CIPM.*

Ion/Atom	Transition	Frequency/ wavelength	Fractional uncertainty
$^{88}\text{Sr}^+$	$5s\ ^2S_{1/2}-4d\ ^2D_{5/2}$	444 779 044 095 484 Hz 674 nm	7×10^{-15}
$^{171}\text{Yb}^+$	$6s\ ^2S_{1/2}-5d\ ^2D_{3/2}$	688 358 979 309 308 Hz 435 nm	9×10^{-15}
$^{199}\text{Hg}^+$	$5d^{10}\ 6s\ ^2S_{1/2}-5d^9\ 6s^2\ ^2D_{5/2}$	1 064 721 609 899 145 Hz 282 nm	3×10^{-15}
^{87}Sr	$5s\ ^2S_{1/2}-4d\ ^2D_{5/2}$	429 228 004 229 877 Hz 698 nm	1.5×10^{-14}

in the relevant publications since additional contributions have been taken into account caused for example by the uncertainty in linking to different Cs clocks.

6.1. Optical frequency standards based on single ions. – The trapping and preparation of ions and their use for frequency standards has been described in detail in a number of reviews and textbooks (see, *e.g.*, [129-132]). An important feature however is the special kind of interrogation of single ions that will be discussed briefly in the following.

6.1.1. Clock interrogation by use of quantum jumps. A properly chosen ion can get close to the ideal situation where a single unperturbed particle at rest is probed. The drawback though is that a single ion does not produce a strong signal by scattering many photons per second on the clock transition. However, the method of quantum jumps or electron shelving proposed by Dehmelt [133,134] and demonstrated later in Wineland's [135] and Dehmelt's group [136] is capable to detect a transition with unity probability. The technique is often applied to so-called V-systems where, as in fig. 14, a strong (cooling)

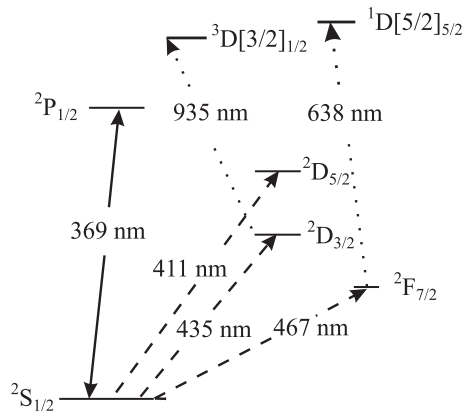


Fig. 14. – Excerpt from the energy level diagram of Yb^+ . The transition at 369 nm is used for cooling the ion and for detecting quantum jumps (see text). Dashed lines (411 nm, 435 nm and 467 nm) represent transitions that were proposed for optical clocks.

transition and a weak (clock) transition are connected at the ground state. When the ion is irradiated by radiation whose frequency is in resonance with the strong transition up to about 10^8 absorption-emission cycles lead to the same number of emitted photons. Even with a limited detection probability of the order of 10^{-3} about 10^5 photons per second can be detected. If, however, the ion is excited on the weak clock transition by resonant radiation, the excited electron is “shelved” in the excited state. Consequently the fluorescence on the strong transition cannot be excited before the ion makes a transition to the ground state again. Thus the fluorescence light from the strong transition monitors the “quantum jumps” of the ion into the excited state and back as sudden intensity changes.

6.1.2. Yb⁺ and Hg⁺ single-ion standards. The clock transitions of the $^{171}\text{Yb}^+$ and $^{199}\text{Hg}^+$ ions given in table I are quadrupole transitions with natural linewidths of 3.1 Hz and 1.1 Hz, respectively. The level scheme of both ions is basically very similar and hence both systems will be treated here at the same time. In Yb⁺ the transition at 369 nm is used for cooling the ion and for detecting quantum jumps. The $^2S_{1/2}$ - $^2D_{3/2}$ transition at 435 nm is preferred, rather than the $^2S_{1/2}$ - $^2D_{5/2}$ transition at 411 nm since the $^2D_{5/2}$ level decay may occur into the long-lived $^2F_{7/2}$ that has a natural lifetime of about ten years. This level is connected to the ground state by an 467 nm octupole clock transition with a natural linewidth of the transition in the nanohertz range [120] and is also investigated as an optical frequency standard.

Two independent $^{171}\text{Yb}^+$ single-ion optical frequency standards operating at the 435 nm line were compared at PTB to look for systematic frequency shifts. A significant contribution to the systematic uncertainty could result from the interaction of the atomic electric quadrupole moment with the gradient of an electric stray field in the trap. Two methods can be used to eliminate the quadrupole shift. One uses the fact that the quadrupole shift averages to zero in three mutually orthogonal directions of the magnetic quantization field [137]. A second method uses the fact that the average over all Zeeman and quadrupole shifts of all magnetic sublevels is zero [138].

Another possible systematic shift can result from the quadratic Stark shift. In the case of the $^{171}\text{Yb}^+$ clock transition the scalar polarizability of the ground state, $\alpha_S(^2S_{1/2})$, and from the scalar and tensorial polarizabilities of the $^2D_{3/2}$ state, $\alpha_S(^2D_{3/2})$ and $\alpha_T(^2D_{3/2})$ contribute to this effect. The contribution has been measured and is corrected for.

For the unperturbed clock transition a mean relative frequency difference of the frequencies between both standards of $(3.8 \pm 6.1) \times 10^{-16}$ was observed [88]. This agreement is similar to that of the most accurate comparisons between cesium fountain clocks. The frequency of the $^{171}\text{Yb}^+$ standard was measured with a relative systematic uncertainty of 3×10^{-15} and a statistical uncertainty of 0.6×10^{-15} using a femtosecond frequency comb generator based on an Er³⁺-doped fiber laser [139].

A similar level scheme of the cooling and clock transitions is present in the optical frequency standard based on the 1.06×10^{15} Hz (282 nm) electric quadrupole transition in a single trapped $^{199}\text{Hg}^+$ ion that was developed at NIST. This frequency standard uses a cryogenic spherical electromagnetic (Paul trap) to trap a single Hg ion for up to 100 days. The frequency measurements over a period of more than five years between the $^{199}\text{Hg}^+$ standard and the Cs primary clock transition agreed to better than 1×10^{-15} over three years [9]. A fractional frequency instability of about 7×10^{-15} at 1 s was demonstrated that follows the $\tau^{-1/2}$ dependence down to the 10^{-17} regime. The uncertainty budget presented from the NIST groups leads to a total fractional uncertainty of 7.2×10^{-17} and represents the smallest uncertainty to find the unperturbed line center reported for an optical clock. This uncertainty is an order of magnitude smaller as the uncertainty

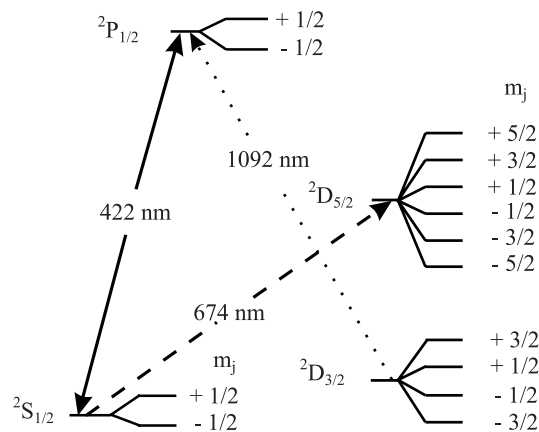


Fig. 15. – $^{40}\text{Sr}^+$ energy level scheme.

of the best cesium atomic clocks. As a result the frequency (in SI Hz) of such an optical clock can never surpass the uncertainty of the latter one.

6.1.3. $^{88}\text{Sr}^+$ single-ion standard. In contrast to the Yb^+ and Hg^+ single-ion standards discussed so far the $^{88}\text{Sr}^+$ $5s\ 2S_{1/2}-4d\ 2D_{5/2}$ at 674 nm 444 779 044 095 484 Hz (fig. 15) of the even isotope is lacking hyperfine structure. Thus there is no magnetic-field insensitive $m_{F=0} \rightarrow m_{F=0}$ transition and a small external field splits the clock transition with a natural linewidth of 0.4 Hz into five pairs of Zeeman components.

This standard is investigated at the British National Physical Laboratory (NPL) [140] and at the National Research Council (NRC) [138] of Canada. In order to eliminate the first-order Zeeman shift, these groups probe alternately a symmetric pair of Zeeman components.

6.2. Neutral atom optical frequency standards. – Neutral-atom-based frequency standards can be divided in three groups: the first one is based on free atoms in an atomic beam effusing from a nozzle and collimated by diaphragms.

6.2.1. Atomic beam standards. The most advanced beam standard in the optical regime are the hydrogen standard based on the $1S-2S$ transition in atomic hydrogen [13, 19, 74] described above and the Ca standard based on the $1S_0-3P_1$ transition (see fig. 16) in atomic Ca [141-143]. The large velocity of the atoms leads to a large second-order Doppler effect which leads to a considerable broadening and shift of the interrogated line. Even though techniques that suppress the first-order Doppler effect were applied, residuals resulting from non-ideal alignment or curvature of the interrogating optical beams (residual first-order Doppler effect) occur that seem to prevent the use of atomic beam for use in optical frequency standards with the highest accuracy.

6.2.2. Neutral atom standards based on ballistic atoms. The large influence of the first- and second-order Doppler effects can be reduced very efficiently by laser cooling the atoms, *e.g.*, in a magneto-optical trap. After shutting off the magneto-optical trap the released atoms have an initial velocity between a few cm/s and a m/s and follow ballistic paths in the gravitational field. Due to the free fall the interrogation of these atoms is

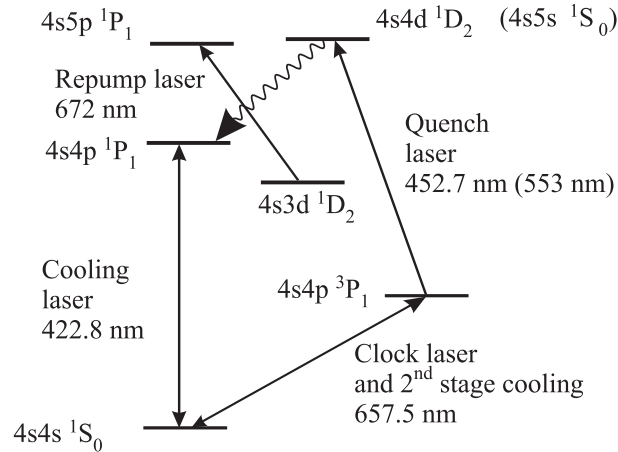


Fig. 16. – Excerpt of the ^{40}Ca energy level scheme. The transition at 423 nm is used for cooling the atoms. The clock transition (657 nm) is also used for second-stage cooling in combination with the quench laser at 423 nm or 553 nm.

limited to a few milliseconds in typical laser beams. The broadening of the interrogated line associated with such an interaction time corresponds to a few hundred hertz. In general, fountain geometries could be utilized to increase the interaction time to about a second [144]. Such a technique has been proposed a long time ago but has never been realized up to now.

For neutral ballistic atom standards therefore mostly alkaline earth atoms like Mg [145], Ca [146-149], Sr [150] have been investigated since there the intercombination transitions 1S_0 - 3P_1 with their natural linewidths between a few tens of hertz and a few kilohertz are well adapted to the achievable interaction time-limited linewidth.

The most investigations and probably the best results have been obtained with calcium. The Ca intercombination transition 1S_0 - 3P_1 (see fig. 16) has a natural width of 0.37 kHz which has been resolved to below the natural linewidth. In [148] a thermal beam of Ca atoms from an oven at 900 K is decelerated using a Zeeman slower from a velocity of 600 m/s to a velocity of about 40 m/s. Then the slow atoms are collimated and deflected by 10 degrees towards a magneto-optical trap (MOT) with a 2D molasses. This set-up avoids the black-body radiation from the hot oven which would lead to a so-called black-body shift [151]. At the first cooling step Ca atoms are cooled on the allowed 423 nm transition 1S_0 - 3P_1 (see fig. 16) and captured in a MOT. In 10 ms about 10^7 atoms are collected in a cloud at a temperature close to the Doppler limit of 0.8 mK for this cooling transition. A second cooling stage is performed using the forbidden 657 nm transition (see fig. 16). For efficient cooling the scattering rate is increased by quenching the upper metastable 3P_1 state by excitation of the 453 nm transition to the $4s4d\ ^1D_2$ state. With this quench cooling method the atoms are further cooled down to 12 μK , corresponding to an r.m.s. velocity of 10 cm/s. Then the clock transition is interrogated using a sequence of four pulses cut from a single cw laser beam. The first pair of pulses and the second one are antiparallel to allow for a first-order Doppler free excitation. The resolution is determined by the time between the first and the second and the third and the fourth pulse. This sequence represents the time domain analogue to the well-known

optical separated field excitation [152] or a Ramsey-Bordé atom interferometer [153]. The necessary radiation to interrogate the clock transition with a spectral linewidth of approximately 1 Hz was provided by a master-slave diode laser system [154].

The frequency of the clock transition at 657 nm was referenced to the caesium fountain clock utilizing a femtosecond comb generator to be 455 986 240 494 144 (5.3) Hz in PTB with a fractional uncertainty of 1.2×10^{-14} and later at NIST with 6.6×10^{-15} [149], one of the lowest uncertainties reported to date for a neutral atom optical standard. These authors also concluded that this type of standard could be capable to achieve a fractional uncertainty in the 10^{-16} regime.

A fractional frequency instability of 4×10^{-15} at 1 s averaging time was achieved. As has been pointed out [39, 146] the quantum projection-noise limit [151] for the Ca standard corresponds to a fractional instability or Allan deviation of $\sigma_y(\tau) < 10^{-16}$ for $\tau = 1$ s. To approach this limit, a frequency instability of the spectroscopy laser of better than 3×10^{-16} for the duration of the atom interferometry $2T \approx 1.3$ ms is necessary since the so-called Dick effect [155] degrades the stability through the aliasing of the laser frequency noise in a discontinuous interrogation. The Dick effect for an optical frequency standard with Ramsey-Bordé interrogation was first addressed by Quessada *et al.* [156]. Hence, the relatively short interaction time achievable with neutral atoms in free flight limits the accuracy and the stability.

6.2.3. Optical lattice clocks. A possible way to combine the advantages of trapped single ions and the large number of neutral atoms, *i.e.* the long storage times and the good signal-to-noise ratio, respectively, was pointed out by Katori [157, 158]. A large array of micro traps for atoms (see fig. 17) can be generated in a standing wave laser field capable of holding maybe a million of atoms. Even though these optical lattices have been investigated for a long time they did not seem to be appropriate to be used in an optical frequency standard because of the large ac Stark shifts associated with the laser field. The remedy for this effect is to tune the lattice laser to a so-called “magic wavelength” where the upper and lower clock levels are shifted by the same amount, leaving the clock transition frequency unaltered (see fig. 18). The big advantage here is that the ac Stark shift can be controlled by controlling the lattice laser frequency rather than by measuring the lattice laser intensity. The former can be determined very accurately, in particular if one has an optical clock at hand.

Several atomic species are investigated for use as lattice clocks, *e.g.*, ^{87}Sr [10, 159-161], Yb [162], and in the future also Hg. The best results have been obtained with ^{87}Sr which will be discussed in the following. The strongly forbidden $J = 0 \rightarrow J = 0$ transition 1S_0 - 3P_0 in Sr (see fig. 19) at 689 nm becomes weakly allowed through hyperfine mixing leading to a natural linewidth of about 1 mHz. The atoms are cooled on the 461 nm transition to several hundred microkelvin. To further reduce the temperature cooling on the 1S_0 - 3P_1 transition is performed before the atoms are transferred into a dipole trap operated at the magic wavelength near 813.4 nm. In a one-dimensional lattice Boyd *et al.* [160] stored typically 2×10^4 atoms distributed across about 80 lattice sites. Interrogating the atoms several effects contribute to the uncertainty to find the unperturbed line center. These authors gave an uncertainty budget where the perturbations due to the residual ac Stark shift of the lattice laser, the effect of the magnetic field necessary to separate the Zeeman levels, and possible collisions contribute the largest effects ending up with a fractional uncertainty below 1×10^{-15} . The frequency of this transition has been determined now by three independent groups [159-161]. The measurement of Boyd *et al.* [160] gave 429 228 004 229 874.0 (1.1) Hz. The associated uncertainty is already much smaller as the

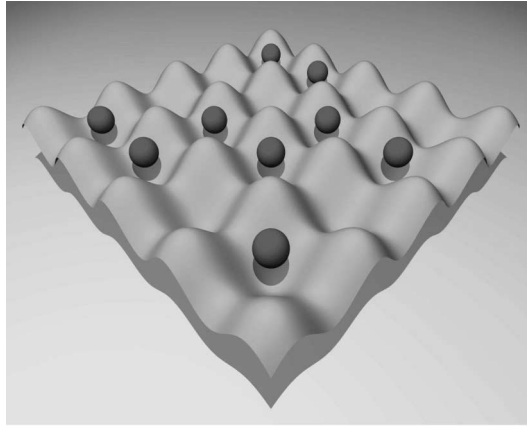


Fig. 17. – Atoms are trapped in the potential minima located at the maxima of a standing wave of the lattice laser.

one recommended very recently by the CIPM (see table I) indicating the current speed of the evolution of optical clocks and frequency standards.

7. – Conclusions

After only a few years the measurement of optical frequencies by optical frequency combs is a mature technology that has led to a variety of novel applications. We are now in a situation where optical frequency standards and clocks are beginning to outperform traditional microwave clocks and most likely will lead in the future to a new definition of the SI unit second probably based on an optical frequency standard. Optical clocks in the

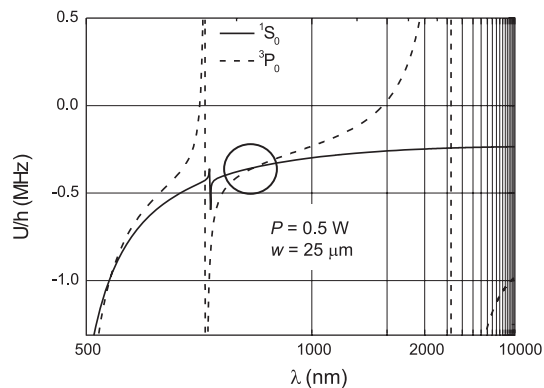


Fig. 18. – The calculated ac Stark shift potential energies U for a given power P and a given waist w of the lattice laser beam for the ground-state 1S_0 and the excited state 3P_0 are equal at the so-called “magic wavelength” (circle).

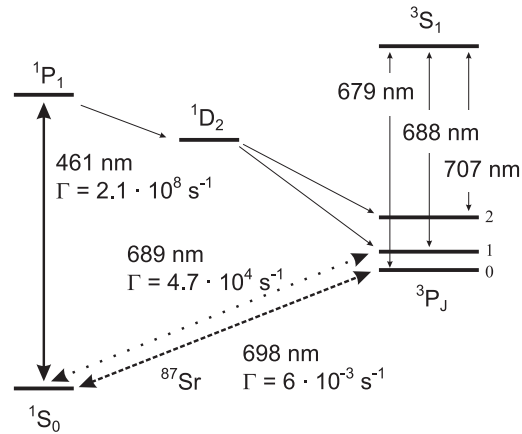


Fig. 19. – Excerpt from the energy level scheme of ^{40}Sr . The transitions at 461 nm and 689 nm are used for cooling the atoms. The dashed line (698 nm) is the clock transition.

visible part of the spectrum by no means need be the end of the evolution. Transitions in the UV or even in the XUV might give superior stability, as this important property scales as the transition frequency in use. It can be expected that the evolution in this field also in the future will keep its current pace since novel ideas like reading out of clock transitions by quantum information techniques [163, 164] or the use of nuclear transitions [165] will continuously shift the frontiers in optical frequency metrology.

REFERENCES

- [1] HALL J. L., *IEEE Sel. Top. Quantum Electron.*, **6** (2000) 1136.
- [2] UDEM TH. *et al.*, in *Proceedings of the 1999 Joint Meeting of the European Frequency and Time Forum and the IEEE International Frequency Control Symposium, Besançon France*, IEEE catalog no. 99CH36313 (1999), pp. 602-625.
- [3] REICHERT J. *et al.*, *Opt. Commun.*, **172** (1999) 59.
- [4] REICHERT J. *et al.*, *Phys. Rev. Lett.*, **84** (2000) 3232.
- [5] DIDDAMS S. A. *et al.*, *Phys. Rev. Lett.*, **84** (2000) 5102.
- [6] JONES D. J. *et al.*, *Science*, **288** (2000) 635.
- [7] HOLZWARTH R. *et al.*, *Phys. Rev. Lett.*, **85** (2000) 2264.
- [8] UDEM TH., HOLZWARTH R. and HÄNSCH T. W., *Nature*, **416** (2002) 233.
- [9] OSKAY W. H. *et al.*, *Phys. Rev. Lett.*, **97** (2006) 020801.
- [10] TAKAMOTO M. *et al.*, *Nature*, **435** (2005) 321.
- [11] GILL P. and MARGOLIS H., *Physics World*, **18** May issue (2005) 35.
- [12] *High Resolution Spectroscopy of Hydrogen*, in *The Hydrogen Atom*, edited by BASSANI G. F., INGUSCIO M. and HÄNSCH T. W. (Springer Verlag, Berlin, Heidelberg, New York) 1989, pp. 93-102.
- [13] NIERING M. *et al.*, *Phys. Rev. Lett.*, **84** (2000) 5496.
- [14] DE BEAUVOIR B. *et al.*, *Eur. Phys. Lett. D*, **12** (2000) 61.
- [15] UDEM TH. *et al.*, *Phys. Rev. Lett.*, **82** (1999) 3568.
- [16] GERGINOV V. *et al.*, *Phys. Rev. A*, **73** (2006) 032504.
- [17] BIZE S. *et al.*, *Phys. Rev. Lett.*, **90** (2003) 150802.
- [18] PEIK E. *et al.*, *Phys. Rev. Lett.*, **93** (2004) 170801.

- [19] ZIMMERMANN M. *et al.*, *Laser Phys.*, **15** (2005) 997.
- [20] KOUROGI M. *et al.*, *IEEE J. Quantum Electron.*, **31** (1995) 2120.
- [21] BROTHERS L. R. and WONG N. C., *Opt. Lett.*, **22** (1997) 1015.
- [22] IMAI K. *et al.*, *IEEE J. Quantum Electron.*, **34** (1998) 1998.
- [23] SPENCE D. E., KEAN P. N. and SIBBETT W., *Opt. Lett.*, **16** (1991) 42.
- [24] DIELS J. C. and RUDOLPH W., *Ultrashort Laser Pulse Phenomena* (Elsevier, Amsterdam, Heidelberg, Tokyo) 2006.
- [25] ECKSTEIN J. N., *High Resolution Spectroscopy using Multiple Coherent Pulses* (Thesis, Stanford University, USA) 1978.
- [26] BASSANI G. F., INGUSCIO M. and HÄNSCH T. W. (Editors) *Frequency Standards in the Optical Spectrum*, in *The Hydrogen Atom*, (Springer Verlag, Berlin, Heidelberg, New York) 1989, pp. 123-133.
- [27] HOLZWARTH R. *et al.*, *Appl. Phys. B*, **73** (2001) 269.
- [28] UDEM TH. *et al.*, *Opt. Lett.*, **24** (1999) 881.
- [29] DIDDAMS S. A. *et al.*, *Opt. Lett.*, **27** (2002) 58.
- [30] MA L. S. *et al.*, *Science*, **303** (2004) 1843.
- [31] STENGER J. and TELLE H. R., *Opt. Lett.*, **25** (2000) 1553.
- [32] KRAUSZ F. *et al.*, *IEEE J. Quantum Electron.*, **28** (1992) 2097.
- [33] HASEGAWA A. and TAPPERT F., *Appl. Phys. Lett.*, **23** (1973) 142.
- [34] AGRAWAL G. P., *Nonlinear Fiber Optics* (Academic Press, New York) 2001.
- [35] SUTTER D. H. *et al.*, *Opt. Lett.*, **24** (1999) 631.
- [36] MORGNER U. *et al.*, *Opt. Lett.*, **24** (1999) 411.
- [37] SIEGMAN A. E., *Lasers* (University Science Books, Mill Valley Ca USA) 1986.
- [38] BRAMWELL S. R., KANE D. M. and FERGUSON A. I., *Opt. Commun.*, **56** (1985) 112.
- [39] HOLLBERG L. *et al.*, see fig. 9 in *IEEE J. Quantum Electron.*, **37** (2001) 1502.
- [40] RUSH D. W., HO P. T. and BURDGE G. L., *Opt. Commun.*, **52** (1984) 41.
- [41] BARTELS A. *et al.*, *Opt. Lett.*, **29** (2004) 1081.
- [42] SWANN W. C. *et al.*, *Opt. Lett.*, **31** (2006) 3046.
- [43] KNIGHT J. C. *et al.*, *Opt. Lett.*, **21** (1996) 1547.
- [44] RANKA J. K. *et al.*, *Opt. Lett.*, **25** (2000) 25.
- [45] RUSSELL P. ST. J., *Science*, **299** (2003) 358.
- [46] BIRKS T. A., WADSWORTH W. J. and RUSSELL P. ST. J., *Opt. Lett.*, **25** (2000) 1415.
- [47] HOLZWARTH R. *et al.*, *Laser Phys.*, **11** (2001) 1100.
- [48] BARTELS A., DEKORSY T. and KURZ H., *Opt. Lett.*, **24** (1999) 996.
- [49] HOI M. *et al.*, *Phys. Rev. Lett.*, **96** (2006) 243401.
- [50] CORWYN K. L. *et al.*, *Phys. Rev. Lett.*, **90** (2003) 113904.
- [51] HOLMAN K. W. *et al.*, *Opt. Lett.*, **28** (2003) 851.
- [52] HOLZWARTH R., PhD thesis Ludwig-Maximilians-Universität Munich (2001).
- [53] DUDLEY J. M. *et al.*, *J. Opt. Soc. Am. B*, **19** (2002) 765.
- [54] ELL R. *et al.*, *Opt. Lett.*, **26** (2001) 373.
- [55] FORTIER T. M. *et al.*, *Opt. Lett.*, **28** (2003) 2198.
- [56] MATOS L. *et al.*, *Opt. Lett.*, **29** (2004) 1683.
- [57] FORTIER T. M. *et al.*, *Opt. Lett.*, **31** (2006) 1011.
- [58] MORGNER U. *et al.*, *Phys. Rev. Lett.*, **86** (2001) 5462.
- [59] DIDDAMS S. A. *et al.*, *IEEE J. Quantum Electron.*, **9** (2003) 1072.
- [60] FUJI T. *et al.*, *Opt. Lett.*, **30** (2005) 332.
- [61] NELSON L. E. *et al.*, *Appl. Phys. B*, **65** (1997) 277.
- [62] KUBINA P. *et al.*, *Opt. Express*, **13** (2005) 909.
- [63] ADLER F. *et al.*, *Opt. Express*, **12** (2004) 5872.
- [64] MCFERRAN J. J. *et al.*, *Opt. Lett.*, **31** (2006) 1997.
- [65] See, for example, GARDENER F. M., *Phase-lock Techniques* (John Wiley & Sons, New York) 1979.
- [66] WALLS F. L. and DEMARCHI A., *IEEE Trans. Instrum. Meas.*, **24** (1975) 210.
- [67] TELLE H. R., in *Frequency Control of Semiconductor Lasers*, edited by OHTSU M. (Wiley, New York) 1996, pp. 137-167.

- [68] BRABEC T., private communication.
- [69] HAUS H. A. and IPPEN E. P., *Opt. Lett.*, **26** (2001) 1654.
- [70] XU L. *et al.*, *Opt. Lett.*, **21** (1996) 2008.
- [71] HELBING F. W. *et al.*, *Appl. Phys. B*, **74** (2002) S35.
- [72] WITTE S. *et al.*, *Appl. Phys. B*, **78** (2004) 5.
- [73] PREVEDELLI M., FREEGARDE T. and HÄNSCH T. W., *Appl. Phys. B*, **60** (1995) S241.
- [74] FISCHER M. *et al.*, *Phys. Rev. Lett.*, **92** (2004) 230802.
- [75] SANTARELLI G. *et al.*, *Phys. Rev. Lett.*, **82** (1999) 4619.
- [76] UZAN J. P., *Rev. Mod. Phys.*, **75** (2003) 403.
- [77] DIRAC P. A. M., *Nature (London)*, **139** (1937) 323.
- [78] WEBB J. K. *et al.*, *Phys. Rev. Lett.*, **87** (2001) 091301.
- [79] MURPHY M. T., WEBB J. K. and FLAMBAUM V. V., *Mon. Not. R. Astron. Soc.*, **345** (2003) 609.
- [80] QUAST R. *et al.*, *Astron. Astrophys.*, **417** (2004) 853.
- [81] SRINAND R. *et al.*, *Phys. Rev. Lett.*, **92** (2004) 121302.
- [82] SHLYAKHTER A. I., *Nature*, **264** (1976) 340.
- [83] FUJII Y. *et al.*, *Nucl. Phys. B*, **573** (2000) 377.
- [84] LAMOREAUX S. K. and TORGERSON J. R., *Phys. Rev. D*, **69** (2004) 121701(R).
- [85] MURPHY M. T. *et al.*, arXiv:astro-ph/0612407v1.
- [86] MURPHY M. T., WEBB J. K. and FLAMBAUM V. V., arXiv:astro-ph/0611080 v3.
- [87] CALMET X. and FRITZSCH H., *Phys. Lett. B*, **540** (2002) 173.
- [88] SCHNEIDER T., PEIK E. and TAMM CHR., *Phys. Rev. Lett.*, **94** (2005) 230801.
- [89] DIDDAMS S. A. *et al.*, *Science*, **293** (2001) 825.
- [90] MOHR P. J. and TAYLOR B. N., *Rev. Mod. Phys.*, **77** (2005) 1.
- [91] GABRIELSE G. *et al.*, *Phys. Rev. Lett.*, **97** (2006) 030802.
- [92] WICHT A. *et al.*, *Phys. Scr.*, **T02** (2002) 82.
- [93] CLADÉ P. *et al.*, *Phys. Rev. Lett.*, **96** (2006) 03301.
- [94] BRADLEY *et al.*, *Phys. Rev. Lett.*, **83** (1999) 4510.
- [95] PACHUCKI K. and JENTSCHURA U. D., *Phys. Rev. Lett.*, **91** (2003) 113005.
- [96] MURPHY M. T. *et al.*, submitted to *Mon. Not. R. Astron. Soc.*
- [97] APOLONSKI A. *et al.*, *Phys. Rev. Lett.*, **85** (2000) 740.
- [98] KIENBERGER R. *et al.*, *Nature*, **427** (2004) 817.
- [99] BALTUŠKA A. *et al.*, *Nature*, **421** (2003) 611.
- [100] WAHLSTRÖM C. G. *et al.*, *Phys. Rev. A*, **48** (1993) 4709.
- [101] BRABEC T. and KRAUSZ F., *Rev. Mod. Phys.*, **72** (2000) 545.
- [102] EDEN J. G., *Prog. Quantum Electron.*, **28** (2004) 197.
- [103] PAULUS G. G. *et al.*, *Phys. Rev. Lett.*, **85** (2000) 253004.
- [104] SERES J. *et al.*, *Nature*, **433** (2005) 596.
- [105] GOULIELMAKIS E. *et al.*, *Science*, **305** (2004) 1267.
- [106] GERGINOV V. *et al.*, *Opt. Lett.*, **30** (2005) 1734.
- [107] FENDEL P. *et al.*, *Opt. Lett.*, **32** (2007) 701.
- [108] BAKLANOV YE. F. and CHEBOTAYEV V. P., *Appl. Phys. Lett.*, **12** (1977) 97.
- [109] MESHULACH D. and SILBERBERG Y., *Nature*, **396** (1998) 239.
- [110] ECKSTEIN J., FERGUSON A. I. and HÄNSCH T. W., *Phys. Rev. Lett.*, **40** (1978) 847.
- [111] SNADDEN M. J. *et al.*, *Opt. Commun.*, **125** (1996) 70.
- [112] MARIAN A. *et al.*, *Science*, **306** (2004) 2063.
- [113] FORTIER T. M. *et al.*, *Phys. Rev. Lett.*, **97** (2006) 163905.
- [114] WITTE S. *et al.*, *Science*, **307** (2005) 400.
- [115] CAVALIERI S. *et al.*, *Phys. Rev. Lett.*, **89** (2002) 133002.
- [116] ZINKSTOK R. TH. *et al.*, *Phys. Rev. A*, **73** (2006) 061801(R).
- [117] GOHLE CH. *et al.*, *Nature*, **436** (2005) 234.
- [118] JONES R. J., MOLL K. THORPE M. and YE J., *Phys. Rev. Lett.*, **94** (2005) 193201.
- [119] BARNES J. A. *et al.*, *IEEE Trans. Instrum. Meas.*, **20** (1971) 105.
- [120] WEBSTER S. A. *et al.*, *Phys. Rev. A*, **65** (2002) 052501.

- [121] See, for example, contributions of MADEJ A. A., BERNARD J. E., RIEHLE F. and HELMCKE J., in *Frequency Measurement and Control*, edited by LUITEN A. N. (Springer Verlag, Berlin, Heidelberg, New York) 2001.
- [122] EVENSON K. M. *et al.*, *Appl. Phys. Lett.*, **22** (1973) 192.
- [123] PEIK E., SCHNEIDER T. and TAMM CHR., *J. Phys. B*, **39** (2006) 145.
- [124] BRUSCH A. *et al.*, *Phys. Rev. Lett.*, **96** (2006) 103003.
- [125] QUINN T. J., *Metrologia*, **40** (2003) 103.
- [126] EDITOR'S NOTE: *Documents concerning the new definition of the metre*, *Metrologia*, **19** (1984) 163.
- [127] QUINN T. J., *Metrologia*, **30** (1993/1994) 523.
- [128] QUINN T. J., *Metrologia*, **36** (1999) 211.
- [129] WINELAND D. J. *et al.*, *Phys. Rev. A*, **36** (1987) 2220.
- [130] BLATT R., GILL P. and THOMPSON R. C., *J. Mod. Opt.*, **39** (1992) 193.
- [131] MADEJ A. A. and BERNARD J. E., *Frequency Measurement and Control: Topics in Applied Physics*, edited by A. N. LUITEN, **79** (2001) 153.
- [132] RIEHLE F., *Frequency Standards: Basics and Applications* (Wiley-VCH, Weinheim) 2004.
- [133] DEHMELT H., *Bull. Am. Phys. Soc.*, **20** (1975) 60.
- [134] WINELAND D. J. and DEHMELT H., *Bull. Am. Phys. Soc.*, **20** (1975) 637.
- [135] WINELAND D. J. *et al.*, *Opt. Lett.*, **5** (1980) 245.
- [136] NAGOURNEY W., SANDBERG J. and DEHMELT H., *Phys. Rev. Lett.*, **56** (1986) 2797.
- [137] ITANO W. M., *J. Res. Natl. Inst. Stand. Technol.*, **105** (2000) 829.
- [138] DUBÉ P. *et al.*, *Phys. Rev. Lett.*, **95** (2005) 033001.
- [139] TAMM CHR. *et al.*, to be published in *IEEE Trans. Instrum. Meas.*
- [140] MARGOLIS H. S. *et al.*, *Science*, **306** (2004) 1355.
- [141] ITO N. *et al.*, *Opt. Commun.*, **109** (1994) 414.
- [142] ZIBROV A. S. *et al.*, *Appl. Phys. B*, **59** (1994) 327.
- [143] KERSTEN P. *et al.*, *Appl. Phys. B*, **68** (1999) 27.
- [144] BEAUSSOLEIL R. G. and HÄNSCH T. W., *Phys. Rev. A*, **33** (1986) 1661.
- [145] STERR U. *et al.*, *Appl. Phys. B*, **54** (1992) 341.
- [146] WILPERS G. *et al.*, *Phys. Rev. Lett.*, **89** (2002) 230801.
- [147] STERR U. *et al.*, *C. R. Physique*, **5** (2005) 845.
- [148] STERR U. *et al.*, *Phys. Rev. A*, **72** (2005) 062111.
- [149] WILPERS G., OAEDES C. W. and HOLLBERG L. W., *Appl. Phys. B*, **85** (2006) 31.
- [150] SORRENTINO F. *et al.*, arXiv:physics/0609133 v1 (2006).
- [151] ITANO W. M. *et al.*, *Phys. Rev. A*, **47** (1993) 3554.
- [152] BORDÉ CH. J. *et al.*, *Phys. Rev. A*, **30** (1984) 1836.
- [153] BORDÉ CH. J., *Phys. Lett. A*, **30** (1989) 10.
- [154] STOEHR H. *et al.*, *Opt. Lett.*, **31** (2006) 736.
- [155] DICK G. J., *Proceedings of 19th Annual Precise Time and Time Interval (PTTI) Applications and Planning Meeting, Redondo Beach, CA, 1987* (U. S. Naval Observatory) 1987, pp. 133-147.
- [156] QUESSADA A. *et al.*, *J. Opt. B: Quantum Semiclassical Opt.*, **5** (2003) S150.
- [157] KATORI H., IDO T. and KUWATA-GONOKAMI M., *J. Phys. Soc. Jpn.*, **68** (1999) 2479.
- [158] KATORI H., in *Proceedings of the 6th Symposium on Frequency Standards and Metrology*, edited by P. GILL (World Scientific, Singapore) 2002, p. 323.
- [159] TAKAMOTO M. *et al.*, *J. Phys. Soc. Jpn.*, **75** (2006) 104302.
- [160] BOYD M. M. *et al.*, *Phys. Rev. Lett.*, **98** (2007) 083002.
- [161] LE TARGAT R. *et al.*, *Phys. Rev. Lett.*, **97** (2006) 130801.
- [162] BARBER Z. W. *et al.*, *Phys. Rev. Lett.*, **96** (2006) 083002.
- [163] WINELAND D. J. *et al.*, in *Proceedings of the 6th Symposium on Frequency Standards and Metrology*, edited by P. GILL (World Scientific, Singapore) 2002, p. 361.
- [164] SCHMIDT P. O. *et al.*, *Science*, **309** (2005) 749.
- [165] PEIK E. and TAMM CH., *Europhys. Lett.*, **61** (2003) 161.